Structure and Function of the Mitochondrial Ribosome

Basil J. Greber[1,*] and Nenad Ban[1]

[1]Department of Biology, Institute of Molecular Biology and Biophysics, ETH Zurich, CH-8093 Zurich, Switzerland; email: ban@mol.biol.ethz.ch

*Present address: California Institute for Quantitative Biosciences (QB3), University of California, Berkeley, California 94720-3220

Annu. Rev. Biochem. 2016. 85:103–32

First published online as a Review in Advance on March 24, 2016

The *Annual Review of Biochemistry* is online at biochem.annualreviews.org

This article's doi: 10.1146/annurev-biochem-060815-014343

Keywords

mitochondrial translation, 39S mitoribosomal subunit, 28S mitoribosomal subunit, antibiotics, ribosome evolution, cryo-electron microscopy

Abstract

Mitochondrial ribosomes (mitoribosomes) perform protein synthesis inside mitochondria, the organelles responsible for energy conversion and adenosine triphosphate production in eukaryotic cells. Throughout evolution, mitoribosomes have become functionally specialized for synthesizing mitochondrial membrane proteins, and this has been accompanied by large changes to their structure and composition. We review recent high-resolution structural data that have provided unprecedented insight into the structure and function of mitoribosomes in mammals and fungi.

Contents

INTRODUCTION

Ribosomes are large ribonucleoprotein complexes that are responsible for protein synthesis in all living cells (1, 2). They are composed of two unequal subunits: The small ribosomal subunit binds messenger RNAs (mRNAs) and translates the encoded message by selecting cognate aminoacyl–transfer RNA (tRNA) molecules (1, 3). The large subunit contains the ribosomal catalytic site termed the peptidyl transferase center (PTC), which catalyzes the formation of peptide bonds, thereby polymerizing the amino acids delivered by tRNAs into a polypeptide chain (4–7). The nascent polypeptides leave the ribosome through a tunnel in the large ribosomal subunit and interact with protein factors that function in enzymatic processing, targeting, and the membrane insertion of nascent chains at the exit of the ribosomal tunnel (5, 8, 9).

Mitochondria are cellular organelles responsible for energy conversion and adenosine triphosphate (ATP) production in eukaryotic cells. In addition to their function in energy metabolism, they play an important part in diverse cellular processes, such as apoptosis (10) and aging (11). Because mitochondria originated from an α-proteobacterial ancestor by endosymbiosis (12, 13), they still contain a strongly reduced mitochondrial genome, as well as mitochondrial ribosomes (mitoribosomes) and other molecular components needed to express the information encoded on the mitochondrial DNA. Even though mitoribosomes are evolutionarily derived from bacterial ribosomes, they have strongly diverged from them in terms of composition (14), function, and structure (15) (**Table 1**). Mitoribosomes have acquired numerous mitochondrial-specific proteins and protein extensions (16–22), and, additionally, their ribosomal RNAs (rRNAs) exhibit considerable plasticity (23–28). These structural changes have been accompanied by a strong functional specialization of the mitoribosome, which synthesizes predominantly, or even exclusively, membrane proteins, including hydrophobic components of highly important complexes of the mitochondrial respiratory chain (29). Consequently, the signal recognition particle targeting system is absent in animal and fungal mitochondria, and mitochondrial ribosomes have become permanently attached to the mitochondrial inner membrane (30–32).

Table 1 Overview of the composition of bacterial, eukaryotic cytosolic, and mitochondrial ribosomes

	Bacteria (*Escherichia coli*) (154)	Eukaryotic cytosol (154)	Mammalian mitochondria (62, 63)	Yeast mitochondria (21, 57)
Ribosome				
Sedimentation coefficient	70S	80S	55S	74S
Molecular weight	2.3 MDa	3.3–4.3 MDa	2.7 MDa	3–3.3 MDa
Number of rRNAs	3	4	3	2
Number of proteins	54	79–80	82	~82[a]
Large subunit				
Sedimentation coefficient	50S	60S	39S	54S
rRNAs	23S (2,904 nt)	26S–28S (3,396–5,034 nt)	16S (1,569 nt)	21S (3,296 nt)
		5.8S (156–158 nt)		
	5S (120 nt)	5S (120–121 nt)	CP tRNA (73–75 nt)	
Number of proteins	33	46–47	52	46
Small subunit				
Sedimentation coefficient	30S	40S	28S	37S
rRNAs	16S (1,534 nt)	18S (1,800–1,870 nt)	12S (962 nt)	15S (1,649 nt)
Number of proteins	21	33	30	~36[a]

Abbreviations: CP, central protuberance; nt, nucleotide; rRNA, ribosomal RNA; tRNA, transfer RNA.
[a]The high-resolution structure of the 37S subunit has not been determined. Therefore, the protein count might change.

Another peculiarity of mammalian mitochondrial translation is the absence of 5′-untranslated regions in the mitochondrial mRNAs (27, 33, 34). Bacterial 5′-untranslated regions harbor the Shine–Dalgarno sequence, which aids in mRNA binding and in the selection of the start codon by base-pairing with the anti-Shine–Dalgarno sequence in the bacterial small subunit rRNA (1, 35). In mammalian mitochondria, this interaction cannot occur, and the selection of the start codon needs to be guided by other features of the mammalian mitoribosomal small subunit or by mitochondrial translation initiation factors (IFs). Additional differences in translation initiation between mitochondria and bacteria—such as the important role of translation activator proteins in yeast mitochondria (36) and the functional replacement of IF1 by an insertion domain in mammalian mitochondrial IF2 (37)—underscore the highly specialized and divergent nature of mitochondrial translation initiation.

Mitochondrial ribosomes have been intensively investigated due to their unique structure and composition and also due to their involvement in human pathologies (38–40), including cardiomyopathies and developmental abnormalities (39, 41–45), cancer (46–48), and hearing loss (ototoxicity) (49). The latter is exacerbated in patients who bear sensitizing mutations in the mitochondrial rRNAs (50), which occur in roughly 0.2–0.3% of the population (51–53).

This review focuses on recent understanding of the structure and function of mitochondrial ribosomes, in particular that gained from data obtained using cryo-electron microscopy (cryo-EM) to determine the structures of mammalian mitoribosomes at near-atomic resolution, which have provided unprecedented insights into the function of mitochondrial ribosomes.

DETERMINATION OF THE STRUCTURE OF MITORIBOSOMES

The first cryo-EM reconstruction of the mammalian 55S mitoribosome was determined in a pioneering effort made by the laboratory of Rajendra K. Agrawal (15, 54) at a resolution of roughly 12–14 Å. This landmark reconstruction revealed a highly divergent overall morphology of the 55S mitoribosome and its 28S small and 39S large subunits compared with the morphology of the bacterial ribosome (15). In agreement with previous rRNA sequence analysis and protein identification made using mass spectrometry (16–20), the rRNA in the 55S mitoribosome was seen to be reduced to an inner core encompassing the functionally important sites, particularly the PTC active site and the decoding site, and large, additional protein masses were observed on its surface (15). As a consequence of the rRNA reduction and the expansion of the mitoribosomal proteome, the intersubunit bridges that hold together the ribosomal subunits have been extensively remodeled, with partial replacement of rRNA bridges by protein-containing bridges (15).

After intense efforts to crystallize mitoribosomes failed to yield crystals suitable for high-resolution structure determination, technical advances in cryo-EM in recent years finally enabled the structure determination of mitoribosomes at substantially improved resolutions. The development of direct electron detectors, which allow for the collection of data that are much improved over those obtained earlier using charge-coupled device cameras (55), led to the determination of the architecture of the mammalian 39S subunit at 4.9 Å resolution in our laboratory (56) and the structure of the yeast 54S large mitoribosomal subunit at 3.2 Å by the laboratories of Venki Ramakrishnan and Sjors Scheres (57). Our interpretation of the 4.9 Å cryo-EM map of the 39S subunit (56) was aided by chemical cross-linking–mass spectrometry (CX–MS) (58), enabling the placement of several mitoribosomal-specific proteins and providing important insights into the overall architecture and membrane association of the 39S subunit. The importance of independent cross-linking constraints in interpreting intermediate-resolution cryo-EM maps was highlighted by a model of the 28S small mitoribosomal subunit at 7 Å resolution that was published by the Agrawal laboratory (59), which showed a number of discrepancies with later, higher-resolution structures. Full atomic models of the mammalian 39S large subunit at 3.4 Å resolution (60, 61), the 28S small subunit at 3.5–3.6 Å resolution (62, 63), and the 55S mitoribosome at 3.5 Å and 3.8 Å resolution (62, 63) were published in late 2014 and early 2015 by both our laboratory (60, 62) and the Ramakrishnan and Scheres groups (61, 63), providing unprecedented insight into the architecture and function of the mammalian mitoribosome.

THE OVERALL STRUCTURE OF THE 55S MITORIBOSOME

The high-resolution cryo-EM reconstructions of the mammalian 39S and 28S subunits and the 55S mitoribosome (60–63) allowed for the tracing and assignment of all mammalian mitoribosomal proteins and the building of near-complete models of the mitoribosomal rRNAs. Because the work was done in parallel in our laboratory (60, 62) and by the Ramakrishnan and Scheres groups (61, 63), small differences exist between the nomenclatures used for ribosomal proteins and intersubunit bridges. We propose using a unified nomenclature for mammalian mitoribosomal proteins that agrees with the recently introduced naming scheme for all ribosomal proteins (64) and serves to disambiguate the discrepancies found in the current literature (**Supplemental Tables 1 and 2**; follow the **Supplemental Material link** in the online version of this article or at **http://www.annualreviews.org/**). We also present a unified nomenclature for the mitoribosomal intersubunit bridges (**Supplemental Table 3**) that takes into account both the human and porcine 55S structures (62, 63). The names for intersubunit bridges that are homologous to bacteria in terms of their localization and involved molecular components are based on the

Supplemental Material

structures of the bacterial 70S ribosome in the canonical and ratcheted states (65, 66), despite the details of the interactions differing slightly. When the structures of mitoribosomes from different species are determined in the future, we propose that for homologous intersubunit bridges, the nomenclature established for mammalian mitoribosomes should be used and that entirely new, mitochondrial-specific bridges should receive unique designations and be numbered sequentially with existing bridge names without overlap.

The high-resolution structures of the mammalian 55S mitoribosome (62, 63) show in detail the strikingly different overall appearance of the mitoribosome from the ancestral bacterial ribosome (**Figure 1*a*,*b***). The rRNA of the mitoribosome is reduced to an innermost core, which is covered by a tightly interacting coat of mitoribosomal proteins that leaves very little rRNA exposed (**Figure 1*c***) and projects far away from the ribosomal core (**Figure 1*a***). Overall, 36 of the 82 proteins in the 55S mitoribosome are mitochondrial-specific, 22 in the large subunit (60) and 14 in the small subunit (63). The interconnectivity of the protein–protein network has increased dramatically from the bacterial to the mammalian mitoribosomes. Whereas bacterial ribosomal proteins have, on average, only 1.5 neighbors, mitoribosomal proteins form contacts with an average of 4.5 neighbors in the yeast 54S large subunit (57) and 4.9 neighbors in the mammalian 39S large subunit (61). The central protuberance (CP) of the 39S subunit is enlarged due to the acquisition of several mitochondrial-specific proteins, and two crescent-shaped pentatricopeptide repeat (PPR)-fold proteins dominate the overall appearance of the 28S small mitoribosomal subunit. The intersubunit bridges between the 39S and 28S subunits in the 55S mitoribosome are less extensive than in bacterial ribosomes, mostly due to the reduction of interacting rRNA segments, and they involve more contacts mediated by proteins (**Figure 1*d*,*e*** and **Supplemental Table 3**). The two mitoribosomal subunits also exhibit considerable conformational flexibility relative to each other. The porcine 55S mitoribosome in complex with mRNA and tRNAs (62) shows a subunit tilting motion (**Figure 1*f***) that differs from both the classical ratcheting movement during tRNA translocation (66, 67) and the more recently discovered subunit rolling that occurs in mammalian cytosolic ribosomes (68). The physiological role of this mode of motion has not been clarified. Both ratcheting and rolling have been observed in the structure of the human 55S mitoribosome without bound mRNA or tRNA ligands (**Figure 1*g***) (63). These observations indicate that mammalian mitoribosomes are able to sample a more extensive conformational space compared with bacterial ribosomes, likely facilitated by the reorganization of intersubunit contacts in mitoribosomes.

Supplemental Material

The functional and structural roles of the mitoribosomal-specific proteins have been longstanding questions in the field. Initially, it had been assumed that the additional proteins in mammalian mitoribosomes functioned as molecular prostheses, replacing missing rRNA segments (14, 69). However, the first cryo-EM reconstruction of the 55S mitoribosome showed that mitoribosomal-specific proteins do not generally fill the volume vacated by rRNA reduction, suggesting that they serve to mediate an expanded functional role rather than act as structural replacements (15). The data on high-resolution structures of the 55S mitoribosome have suggested that mitoribosomal-specific proteins can, in fact, serve both roles: providing additional functionality, such as membrane association (56) and mRNA recruitment (62, 63), and structurally compensating for the interactions mediated by missing rRNA segments, as observed in the region around uL24m (**Figure 1*b–j***) (56). In bacterial ribosomes, uL24 forms extensive interactions with domain I of the 23S rRNA (**Figure 1*j***) (5, 65). However, these rRNA segments are mostly missing in the 16S rRNA of the 39S subunit, and the interactions they engage in with uL24 in bacteria are replaced in the mammalian mitoribosome by protein–protein contacts with mL45 and uL29m (**Figure 1*i***) (56, 60). This exchange of contacts likely occurred in a stepwise fashion, in which protein–protein contacts were gradually formed, thus permitting the reduction of rRNA contacts without impairing uL24 binding and mitoribosomal structure.

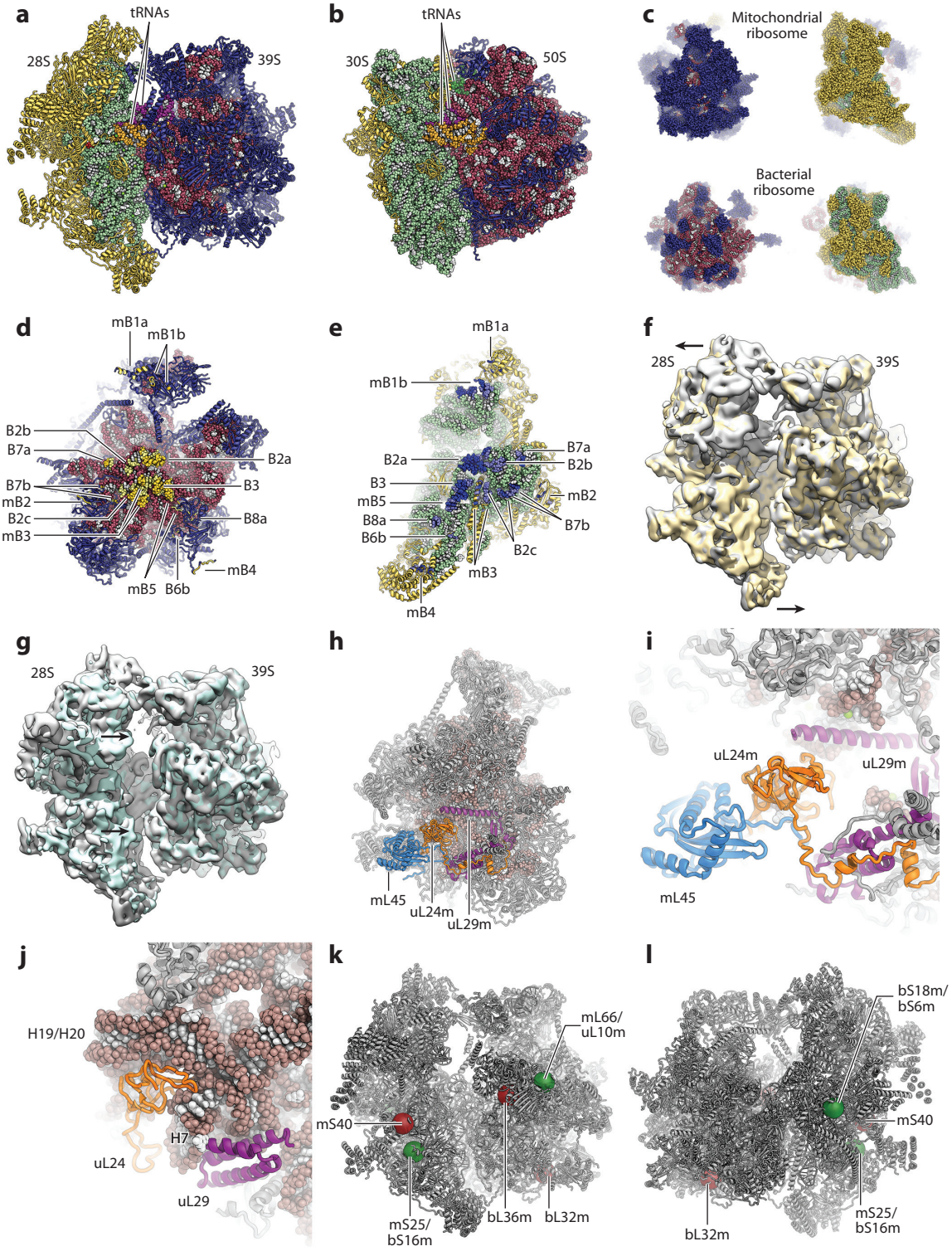
a
tRNAs
28S
39S
b
tRNAs
30S
50S
c
Mitochondrial ribosome
Bacterial ribosome
d
mB1a
mB1b
B2b
B7a
B2a
B7b
B3
mB2
B2c
B8a
mB3
mB4
mB5
B6b
e
mB1a
mB1b
B7a
B2a
B2b
B3
mB2
mB5
B8a
B7b
B6b
B2c
mB3
mB4
f
28S
39S
g
28S
39S
h
mL45
uL24m
uL29m
i
uL24m
uL29m
mL45
j
H19/H20
H7
uL24
uL29
k
mL66/
uL10m
mS40
mS25/
bS16m
bL36m
bL32m
l
bS18m/
bS6m
mS40
bL32m
mS25/
bS16m

Zinc-binding motifs, in which more than one protein chain contributes to the coordination of a single zinc ion, are an unusual feature found in several mitoribosomal proteins (**Figure 1*k*,*l***) (62, 63). Such motifs occur in mL66 and bS18m, two homologs of the bacterial ribosomal protein bS18, where uL10m and bS6m contribute one of the zinc-binding residues, as well as between bS16m and mS25. Even though such interactions have been observed before (70), their increased frequency of occurrence in the 55S mitoribosome suggests that they may have evolved to stabilize the structures and quaternary interactions of rapidly evolving mitoribosomal proteins.

The mRNA, as well as A- and P-site tRNAs, are visible in the intersubunit space of the structure of the porcine 55S mitoribosome (**Figure 1*a***) (62), indicating that this structure represents a mitoribosome stalled during translation. The conformation of the PTC in this structure corresponds to the activated state, with accommodated A- and P-site substrates (60), as has been observed in bacterial ribosomes with bound mRNA and tRNAs (71). It remains to be elucidated why these ribosomal particles are trapped with classical A- and P-site tRNAs rather than in a state after peptidyl transfer and formation of tRNA hybrid states. The density of the nascent polypeptide chain can be seen in the polypeptide exit tunnel of both the porcine and the human 39S subunit structures (60, 61), even though the latter does not contain a P-site tRNA. The nascent chain density unambiguously assigns the path of the polypeptide exit tunnel in the mammalian mitoribosome, confirming that it is highly similar to the path of the bacterial tunnel (60, 61) but different from the proposed nascent polypeptide exit path in the yeast counterpart (**Figure 2**) (57). The mitoribosomal tunnel appears to be tailored for the synthesis of hydrophobic membrane proteins because its walls are more hydrophobic compared with those of the bacterial tunnel, thereby providing contact surfaces for interactions with unfolded, egressing polypeptides (61).

AN ARCHITECTURAL tRNA IN THE 39S SUBUNIT CENTRAL PROTUBERANCE

The CP in bacterial, archaeal, and eukaryotic cytosolic ribosomes is assembled around the 5S rRNA, which acts as a structural scaffold to which a number of ribosomal proteins bind (5, 65, 72, 73). The CP is a functional landmark of the large subunit because it mediates intersubunit contacts to the small subunit, as well as contacts to the tRNAs bound in the intersubunit space (65). There is no 5S rRNA gene in the yeast or mammalian mitochondrial genome, suggesting that the 5S rRNA is absent from their mitoribosomes. In agreement with this notion, the first cryo-EM structure of the mammalian mitoribosome showed no density corresponding to the 5S rRNA (15). Nevertheless, the presence or absence of the 5S rRNA in mammalian mitoribosomes has been controversial because biochemical evidence suggests that, indeed, 5S rRNA is imported

Figure 1

Overview of the mammalian 55S mitoribosome structure. Comparison of the (*a*) mammalian 55S mitoribosome (PDB identification number 5AJ4) with the (*b*) bacterial 70S ribosome (PDB identification number 4V5D). (*c*) The surface of the 55S mitoribosome is mostly covered by proteins, but on the surface of the bacterial 70S ribosome much rRNA is exposed. (*d*) Intersubunit bridges of the 39S subunit are colored yellow, and (*e*) those of the 28S subunit are blue. (*f*,*g*) Intersubunit motions observed in porcine and human 55S structures. In addition to the canonical intersubunit rotation, the 55S mitoribosome exhibits (*f*) tilting and (*g*) rolling movements. The direction of movement is indicated by arrows. (*h–j*) Remodeling of rRNA–protein contacts in the mammalian mitoribosome. (*h*,*i*) In the mammalian mitoribosome, uL24m (*orange*) is held in place by contacts to uL29m (*purple*) and mL45 (*blue*), which replace extensive rRNA contacts in (*j*) the bacterial 70S ribosome. (*k*,*l*) Zinc-finger proteins in the 55S mitoribosome. In addition to canonical zinc-finger motifs (*red spheres*), the 55S contains several zinc-binding motifs (*green spheres*) where multiple proteins are involved in binding a single zinc ion. Abbreviations: PDB, Protein Data Bank; rRNA, ribosomal RNA; tRNA, transfer RNA.

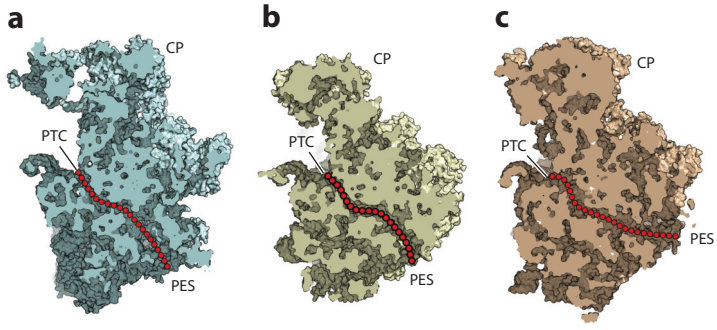

Figure 2

The mitoribosomal polypeptide exit tunnel. Polypeptide tunnel paths in the subunits are indicated by a dotted red line for the (*a*) mammalian 39S (PDB identification numbers 4V19 and 4V1A), (*b*) bacterial 50S (PDB identification number 4V5D), and (*c*) yeast 54S (PDB identification number 3J6B) subunits. Abbreviations: CP, central protuberance; PDB, Protein Data Bank; PES, polypeptide exit site; PTC, peptidyl transferase center.

from the cytosol into mammalian mitochondria, where it might assemble into mitoribosomal particles (74–76).

The first clues toward resolving this apparent discrepancy came from our 4.9 Å resolution cryo-EM reconstruction of the 39S subunit, which showed an area of density exhibiting the characteristic shape of an RNA stem-loop at the CP in a location close to the position of domain β of 5S rRNA in bacteria (**Figure 3*a***) (56). However, the density was inconsistent with the presence of full-length 5S rRNA. Strikingly, this unknown RNA molecule was eventually identified as an architectural tRNA molecule, termed CP tRNA, in the 3.4 Å resolution structures of the 39S subunit from pigs and humans (**Figure 3*b*,*c***) (60, 61). We reported the presence of mitochondrial $tRNA^{Phe}$ based on the identification of the sequence of purines and pyrimidines in our cryo-EM density maps of the porcine 39S subunit (60), and the Ramakrishnan and Scheres groups (61) identified mitochondrial $tRNA^{Val}$ in RNA sequencing experiments using samples from human cell cultures. It remains to be established whether this discrepancy is due to the species- or tissue-specific incorporation of different tRNAs into the structure of the 39S subunit. Interestingly, both mitochondrial $tRNA^{Phe}$ and mitochondrial $tRNA^{Val}$ are encoded in the immediate vicinity of the mitochondrial 12S and 16S rRNA genes in the mitochondrial genome (27), and they are expressed in the same operon as the rRNAs (77). Therefore, they are likely to be present in sufficient amounts for stoichiometric incorporation into the mitoribosome.

The CP tRNA forms extensive interactions with several mitoribosomal proteins at the CP (**Figure 3*c***). Therefore, it likely serves as an architectural replacement for the bacterial 5S rRNA (**Figure 3*d*,*e***) and functions as a stable structural scaffold to organize the structure of the CP (60). Interestingly, protein uL18m in the 39S subunit CP, and its homolog uL18 in the 50S subunit, binds to the CP tRNA and the 5S rRNA in a similar manner (**Figure 3*d***) (5, 60). In the yeast 54S subunit, which contains neither CP tRNA nor uL18m (57), an rRNA expansion segment in this area may have an architectural role similar to that of the CP tRNA (**Figure 3*c*,*f***) (60).

INTERACTIONS OF THE MITORIBOSOME WITH tRNA AND mRNA

Mitochondrial tRNAs exhibit considerable variability in their elbow regions, particularly due to sequence-length variations of the D- and T-stems (78). The ribosomal elements interacting with these tRNA regions are largely missing in mammalian mitoribosomes, where in the A-site,

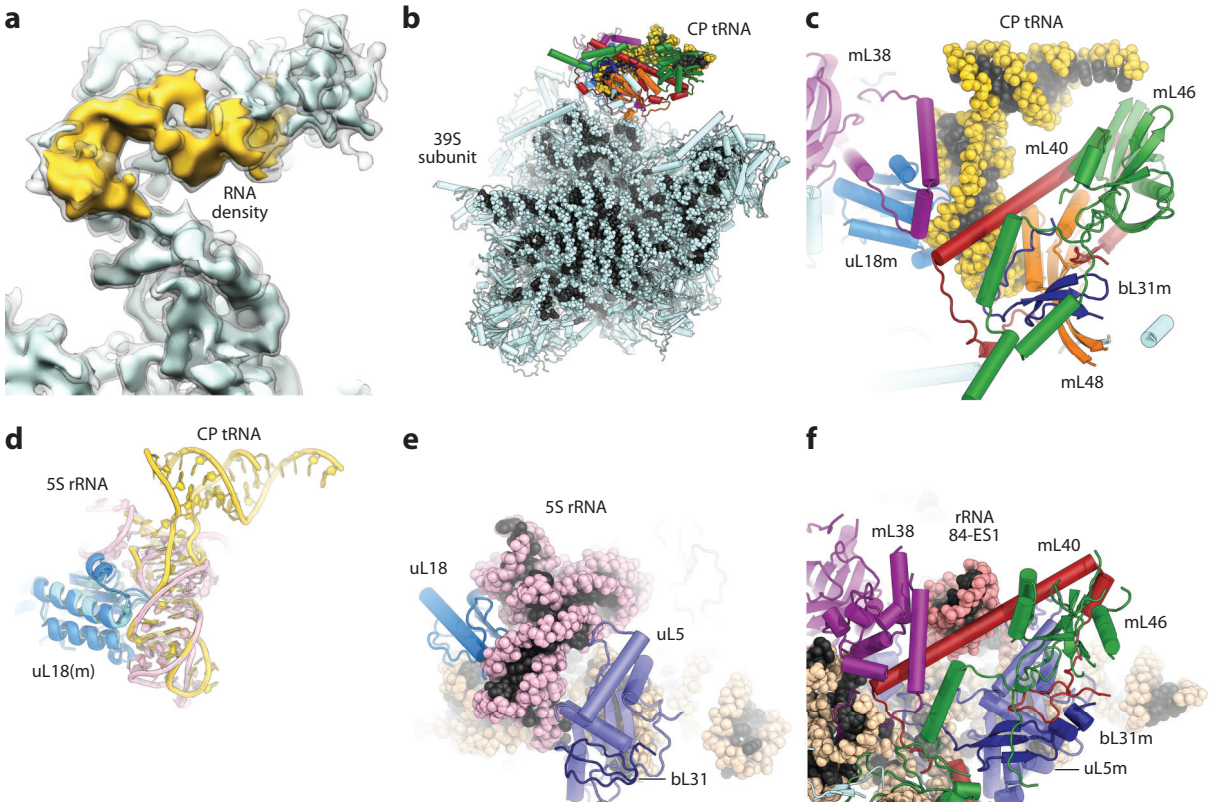

Figure 3

The CP tRNA in the mammalian 39S subunit. (*a*) Cryo-EM map of the 39S subunit at 4.9 Å (EMD identification number 2490) suggesting the presence of an RNA molecule (*yellow*) at the CP. (*b*) Overview of the 39S structure (PDB identification numbers 4V19 and 4V1A) with the CP tRNA highlighted in yellow. (*c*) The CP tRNA in the 39S subunit organizes the CP architecture by serving as a binding site for several mitoribosomal proteins. (*d*) Superposition of the bacterial 5S rRNA–uL18 complex (*pink* and *light blue*; PDB identification number 4V5D) and the mitoribosomal CP tRNA–uL18m complex (*yellow* and *blue*; PDB identification numbers 4V19 and 4V1A). The RNA molecule is bound similarly by uL18(m) in both cases, positioning the anticodon stem-loop of the CP tRNA in the region of domain β of the 5S rRNA. (*e*,*f*) Comparison of the CP architecture of the bacterial 50S and yeast mitochondrial 54S subunits (PDB identification number 3J6B). An rRNA expansion segment partially assumes the role of CP tRNA/5S rRNA in the 54S subunit by providing binding surfaces for mitochondrial proteins conserved between yeast and mammals. Abbreviations: CP, central protuberance; cryo-EM, cryo-electron microscopy; EMD, Electron Microscopy Data Bank; PDB, Protein Data Bank; rRNA, ribosomal RNA; tRNA, transfer RNA.

uL25m and rRNA helix H38 (also termed the A-site finger) are missing, and in the P-site, uL5m and H84 have been lost (61). The interactions of the conserved parts of the tRNAs—including the CCA–3′ acceptor ends and the anticodon stem-loops, which interact with the decoding site on the small subunit and the PTC of the large subunit—are mostly conserved because of their critical importance in the most fundamental ribosomal functions (60, 62, 63).

A unique mitoribosomal structural element, termed the P-site finger (15), emanates from the 39S subunit CP and contacts both the A- and P-site tRNAs (**Figure 4*a***) (60, 62). It likely serves to compensate for the ribosome–tRNA interactions lost due to the absence of the A-site finger in the mitoribosomal A-site and uL5 in the P-site. The P-site finger appears to consist of two α-helices

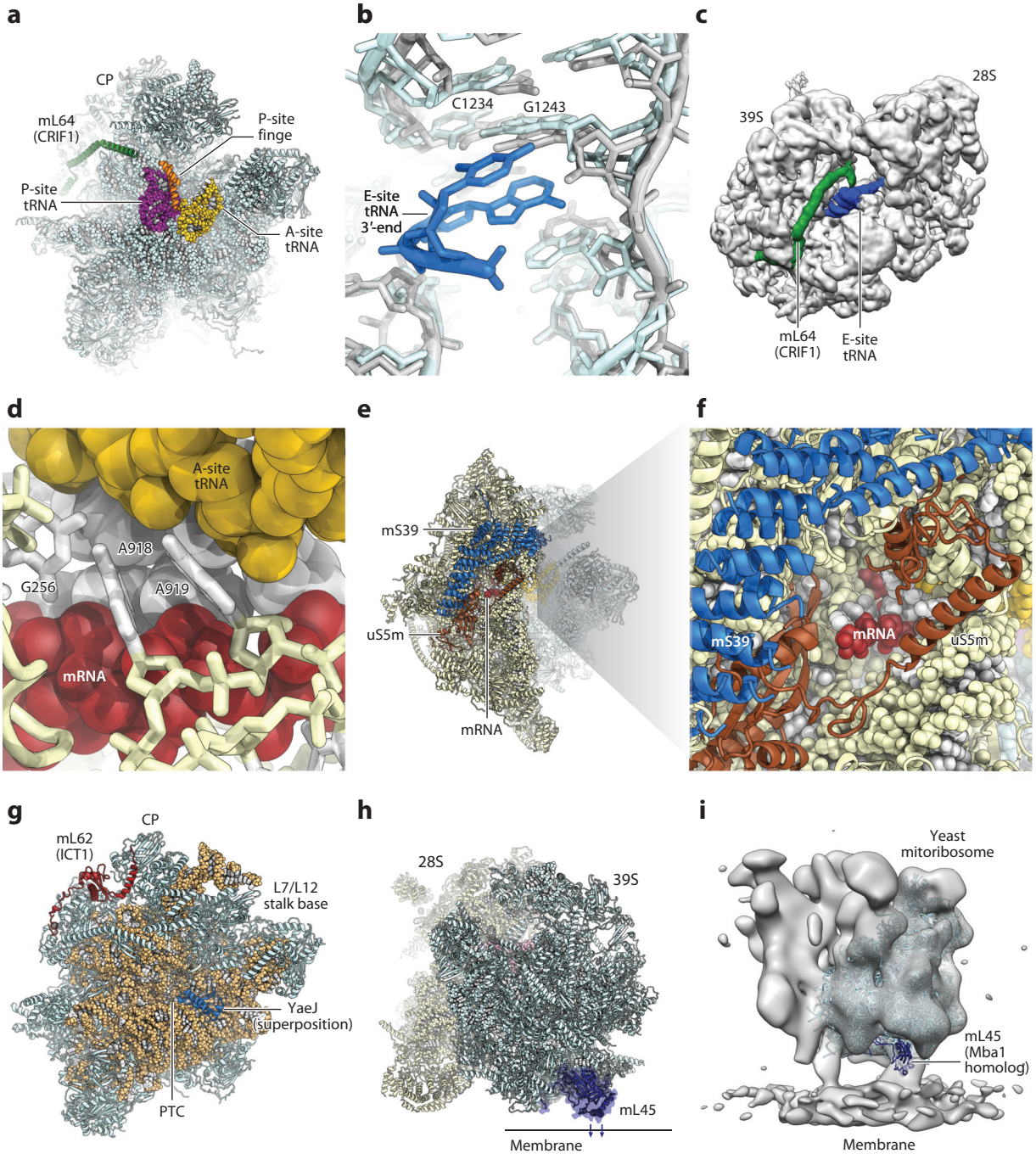
a
CP
mL64
(CRIF1)
P-site
finge
P-site
tRNA
A-site
tRNA
b
C1234
G1243
E-site
tRNA
3′-end
c
28S
39S
mL64
(CRIF1)
E-site
tRNA
d
A-site
tRNA
A918
G256
A919
mRNA
e
mS39
uS5m
mRNA
f
mS39
mRNA
uS5m
g
CP
mL62
(ICT1)
L7/L12
stalk base
YaeJ
(superposition)
PTC
h
28S
39S
mL45
Membrane
i
Yeast
mitoribosome
mL45
(Mba1
homolog)
Membrane

that connect to the CP near mL40 and mL48 (60); however, their exact identity has not yet been assigned due to the low local resolutions of the cryo-EM reconstructions in this area (62).

Based on sequence analyses and the absence of detectable E-site tRNA occupancy in the earliest 55S mitoribosome cryo-EM reconstructions, it had been proposed that the E-site in the mitoribosome was entirely absent or very weak (15, 54, 79). In bacteria, the E-site is important for the fidelity of decoding and for maintaining the reading frame during translation (80, 81). However, our structure of the 39S subunit (60) showed that the E-site nucleotides forming the binding pocket of the CCA–3′-end of the E-site tRNA, including the base pair G1243–C1234 (G2421–C2395 in bacteria), which is crucial for E-site tRNA binding (82), are highly conserved in both sequence and structure (**Figure 4*b***). Consequently, the 39S subunit and 55S mitoribosome structures from the Ramakrishnan and Scheres labs (61, 63), as well as recent data from the Agrawal lab (83), have shown an E-site tRNA in the cryo-EM density map (**Figure 4*c***). Mitoribosomal protein mL64 (CRIF1) may interact with E-site tRNAs bound in the mammalian mitoribosome, as connecting density has been visualized in the cryo-EM maps of the human 55S mitoribosome (**Figure 4*c***) (63).

The decoding site, where the A-site tRNA interacts with the mRNA, is an important functional center of the small ribosomal subunit. In our structure of the 55S mitoribosome in complex with mRNA and tRNA, the locations of base pairs between the A- and P-site tRNA anticodons and the mRNA codons are clearly recognizable. The important bases A918 and A919 (corresponding to bacterial A1492 and A1493) form A-minor interactions with the codon–anticodon helix in the mitoribosomal A-site (**Figure 4*d***) (62), as has been observed after the binding of a cognate tRNA in the bacterial A-site (3). The interaction of G256 (bacterial G530) with the codon–anticodon helix (3) is also conserved between the mitochondrial and bacterial decoding centers (**Figure 4*d***) (62). In summary, these observations suggest that the mechanism of decoding is highly conserved between mammalian mitochondrial and bacterial ribosomes.

Although the central parts of the mitoribosomal mRNA channel, including the A- and P-sites, are relatively well conserved (62), the need to recruit the leaderless mitochondrial mRNAs (27, 33, 34) to the 28S subunit during translation initiation resulted in structural adaptations in the mammalian mitoribosome. The mRNA entry site of the 28S subunit is substantially remodeled compared with that of bacterial ribosomes. In particular, protein uS4 and a domain of uS3, implicated in mRNA helicase activity in bacteria (84), are missing in the mammalian mitoribosome (63).

←

Figure 4

Functional centers of the mitoribosome. (*a*) The P-site finger (*orange*) contributes to P- and A-site tRNA binding in the 39S subunit (PDB identification number 5AJ4), and mL64 (CRIF1) may contact the E-site tRNA (see panel *c*). (*b*) Binding of the 3′-terminal two nucleotides of the E-site tRNA (*blue*; PDB identification number 3J9M) to the 39S E-site (*cyan*; bacterial structure in *gray*). The critical C1234–G1243 base pair is conserved between bacteria and mitochondria. (*c*) The E-site tRNA (*blue*) is visible in this low-pass filtered cryo-EM map of the human mitoribosome (EMD identification number 2876). A density (*green*), most likely belonging to mL64 (CRIF1), can be seen to contact the E-site tRNA. (*d*) Decoding in the 28S subunit. The highly conserved bases A918, A919, and G256 proofread the minor groove of the codon–anticodon helix formed by mRNA (*red*) and the A-site tRNA (*yellow*). (*e*,*f*) Proteins mS39 (*blue*) and uS5m (*brown*) near the mRNA (*red*) channel entrance. Protein mS39 sits above the channel entrance and may be involved in mRNA recruitment, and uS5m forms a latch across the mRNA channel. (*g*) In the structure of the 39S subunit, the peptidyl-tRNA hydrolase mL62 (ICT1) (*red*) is located >80 Å from the usual binding site of peptidyl-tRNA hydrolases in the A-site (bacterial YaeJ superposed in *blue*; PDB identification number 4V95). (*h*) Mitoribosomal-specific protein mL45 (*dark blue*) is located in the vicinity of the polypeptide tunnel exit and mediates the association of the mitoribosome (*cyan*, large subunit; *yellow*, small subunit) with the mitochondrial inner membrane (*arrows*; the membrane plane is schematically indicated). (*i*) Cryo-EM tomographic reconstruction of the yeast mitoribosome (EMD identification number 2826) bound to membranes (*cyan*, yeast 54S structure; PDB identification number 3J6B; *dark blue*, superposed mL45 from the 39S structure). Abbreviations: CP, central protuberance; cryo-EM, cryo-electron microscopy; EMD, Electron Microscopy Data Bank; PDB, Protein Data Bank; PTC, peptidyl transferase center; tRNA, transfer RNA.

A mitochondrial extension of uS5m connects the 28S subunit body and head domains, thereby forming a latch across the mRNA channel, and this may partially replace the missing residues of uS4 in this area (**Figure 4*e*,*f***) (62, 63). Whether the 28S subunit retains mRNA helicase activity remains to be determined. The PPR-fold protein mS39 is located close to the entry of the mRNA channel and may aid in the recruitment of mRNAs and their threading into the mRNA channel (**Figure 4*e*,*f***) because mS39, like other PPR folds (85, 86), has been shown to bind RNA (87, 88), and its knock down impairs mitochondrial protein synthesis (87).

STRUCTURAL AND CATALYTIC ROLES OF THE MITOCHONDRIAL PEPTIDYL-tRNA HYDROLASE ICT1

At the end of protein synthesis, class 1 release factors bind to the A-site of the terminating ribosome to hydrolyze the ester bond between the P-site tRNA and the nascent chain. The hydrolysis reaction is catalyzed by the insertion of a conserved GGQ motif into the ribosomal PTC (89, 90). Mammalian mitochondria contain four different class 1 release factors: mtRF1, mtRF1a, ICT1 (immature colon carcinoma transcript 1, also termed mL62, see below), and C12orf65. However, mtRF1a may be able to terminate protein synthesis on all mitochondrial mRNAs by recognizing the UAA and UAG stop codons. According to this hypothesis, the nonstandard AGA and AGG codons, for which no cognate tRNAs exist in mitochondria, are converted into UAG stop codons by a −1 frameshift to enable translation termination (91). The roles of the other mitochondrial members of the class 1 release-factor family, including ICT1, have not yet been conclusively established. Interestingly, ICT1 has been found to be a stably incorporated component of the mitoribosomal 39S subunit, where it is termed mL62, and where it has been suggested to act as a codon-independent peptidyl-tRNA hydrolase to rescue stalled mitoribosomes after premature abortion of translation (92). This activity depends on its catalytic GGQ motif, which is essential for cell viability (92). The incorporation of mL62 (ICT1) into the mitoribosome has been hypothesized to be a means of regulating the otherwise uncontrolled, codon-independent activity of the protein in peptidyl-tRNA hydrolysis (92).

However, our structural analyses of the porcine 39S subunit (56, 60) revealed that mL62 (ICT1) in the mitoribosome is located >80 Å away from the site of action of typical peptidyl-tRNA hydrolases, which bind to the A-site (**Figure 4*g***), indicating that mL62 (ICT1) in the 39S subunit might perform a structural role, and soluble copies of the protein would perform peptidyl-tRNA hydrolysis (56). In agreement with these structural findings, biochemical experiments have revealed that ribosome-integrated mL62 (ICT1) is catalytically inactive, and that peptidyl-tRNA hydrolysis is performed by soluble ICT1, which binds to mammalian 55S mitoribosomes (93). Furthermore, these experiments have suggested that in addition to its role as a rescue factor, ICT1 may act to terminate mitochondrial translation at the nonstandard AGA and AGG termination codons, obviating the need for −1 ribosomal frameshifting and establishing a role for ICT1 in canonical translation termination in mitochondria (93). Further experimentation will be required to determine whether mitochondrial translation termination at the AGA and AGG codons in vivo is performed by ICT1 (94) or by mtRF1a after −1 frameshifting (95).

MEMBRANE ASSOCIATION OF MITORIBOSOMES AND ADAPTATIONS OF THE TUNNEL

Mammalian mitoribosomes synthesize 13 proteins, all of them highly hydrophobic membrane protein components of the mitochondrial respiratory chain. The yeast mitoribosome is similarly specialized for membrane protein production, as only one of the proteins it synthesizes is soluble,

the remainder being membrane proteins (29). Early experiments with mammalian mitoribosomes indicated that a significant fraction of them is stably associated with membranes independent of the presence of a nascent chain (30). This suggested that specialized proteins that anchor the mitoribosome to the membrane exist. Steric constraints would dictate that such a membrane anchor protein would be localized close to the exit of the polypeptide tunnel to optimally position the mitoribosome for membrane insertion of newly synthesized proteins.

Genetic and biochemical analyses in yeast have suggested that the protein Mba1 is involved in the membrane attachment of the mitoribosome because its deletion impairs membrane protein insertion (31, 96) and because Mba1 shows homology to the C-terminal domain of TIM44 (97, 98), which is known to mediate membrane association. Indeed, our 4.9 Å structure of the mammalian 39S subunit revealed that mL45, the mammalian homolog of Mba1, is located next to the tunnel exit of the mammalian mitoribosome (**Figure 4*b***), suggesting that it is one of the membrane anchor proteins that help attach the mitoribosome to the membrane (56). Subsequent cryo-EM tomography experiments from the Friedrich Förster laboratory (32) have been in excellent agreement with this hypothesis (**Figure 4*i***). Therefore, mammalian mL45 and yeast Mba1 likely have a major conserved role in the membrane attachment of mitoribosomes that is possibly supported by additional protein– or rRNA–membrane interactions (32), which may involve Mdm38 in yeast or Letm1 in mammals (99).

In addition to the recruitment of membrane anchor proteins to the mitoribosome near the polypeptide exit site, the polypeptide tunnel wall itself may also have become adapted to synthesize membrane proteins, as the Ramakrishnan and Scheres groups (61) have visualized several interactions between the EM density of a polypeptide chain trapped in the tunnel and hydrophobic residues of the tunnel wall, mainly from uL22m.

BINDING OF ANTIBIOTICS TO MITORIBOSOMES

The ribosome is a target for a variety of clinically important antibiotics (100). Due to structural differences between various classes of ribosomes, many antibiotics affect bacterial, eukaryotic cytosolic, and mitochondrial ribosomes differently. Indeed, clinically useful antibiotics should target bacterial ribosomes with high specificity and without inhibiting cellular translation.

Macrolide antibiotics, such as erythromycin, bind inside the polypeptide tunnel of the large ribosomal subunit (101, 102). The entrance to the polypeptide tunnel of the yeast 54S large mitoribosomal subunit shows a strong constriction close to the erythromycin-binding site (**Figure 5*a***), which likely precludes the antibiotic from binding, thus explaining the resistance of yeast mitoribosomes to macrolides (57). Mammalian mitoribosomes also show resistance to erythromycin binding (103, 104), even though they do not contain the constriction at the entrance to the polypeptide tunnel that is observed in yeast mitoribosomes (**Figure 5*b***) (60, 61). Rather, their tunnel shape resembles the one present in bacterial, archaeal, and eukaryotic cytosolic ribosomes, in which the binding of erythromycin depends on the nature of the single nucleotide at position 2058 (*Escherichia coli* sequence numbering) of the large subunit rRNA. Because mammalian mitoribosomes carry a G at the corresponding position (**Figure 5*c***), resistance is probably conferred by the same mechanism as has been established for eukaryotic cytosolic and archaeal ribosomes, in which the presence of a G interferes with erythromycin binding (72, 105). The single G-to-A base substitution has been shown to render archaeal ribosomes susceptible to erythromycin binding, but the presence of an A at this position in bacterial ribosomes is compatible with erythromycin binding (101), and the A-to-G substitution confers resistance (105).

Aminoglycosides bind to the small ribosomal subunit and are used to treat bacterial infections due to their bactericidal effect. Additionally, they have also been developed to treat human

congenital diseases that are caused by premature stop codons, as they can increase stop codon read-through (106). Aminoglycosides can bind to the ribosome at several binding sites (107), most importantly in a pocket in rRNA helix h44 near the decoding center (**Figure 5*d*,*e***) (100, 108, 109). Many aminoglycosides exhibit lower affinity for the mitoribosomal 28S subunit than for bacterial ribosomes because this binding pocket is structurally altered in the mitochondrial 12S rRNA, where two base pairs present in bacteria are turned into the mitochondrial A916–C854 and C917–C853 mismatches (**Figure 5*f–b***) (50, 110). However, sensitizing mutations in patients' mitochondrial 12S rRNA, such as the human mitochondrial A1555G and C1494T mutations

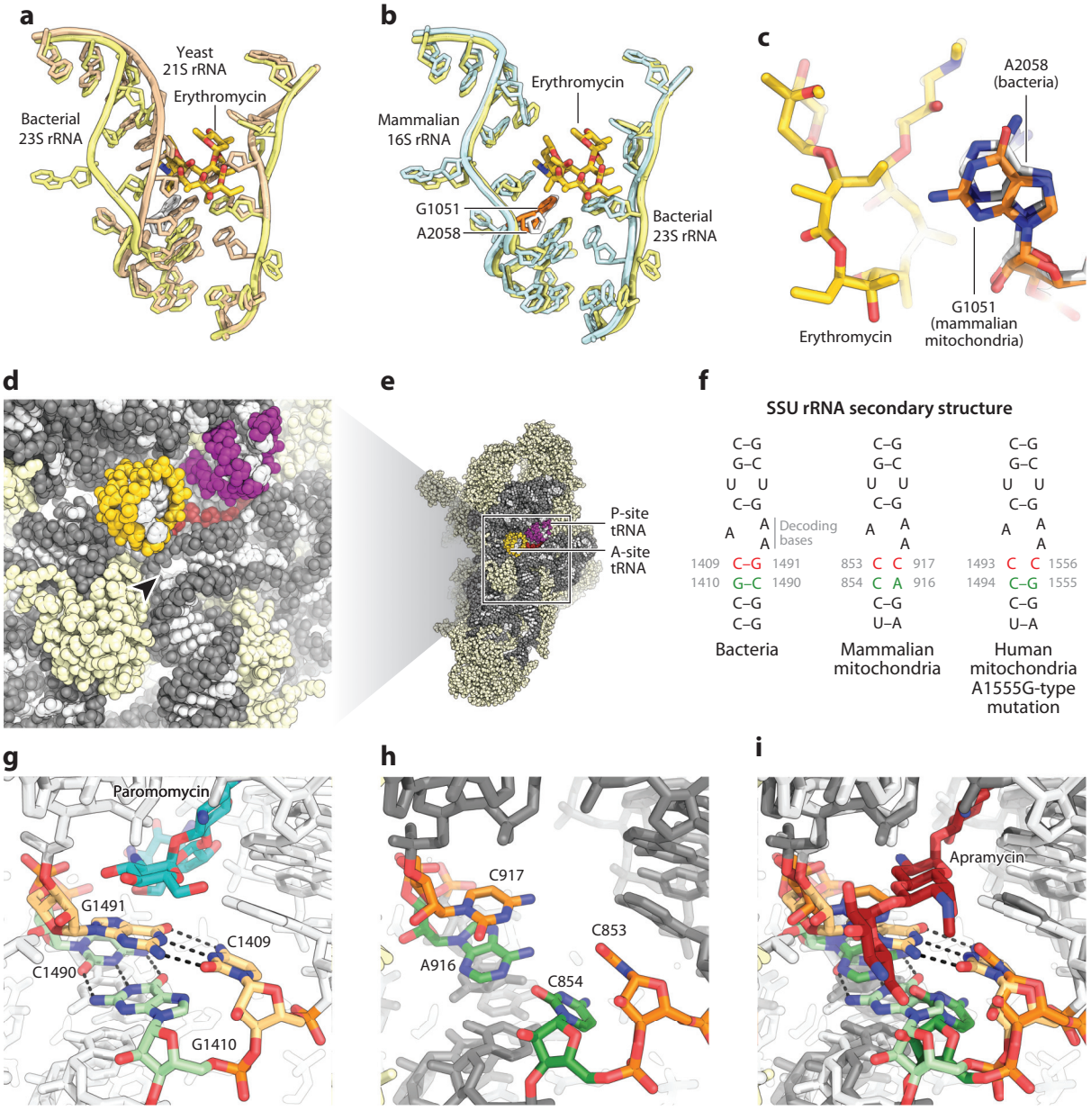

(38, 49) (A916G and C854U in the porcine 12S rRNA), reestablish one of the lost bacterial-like base pairs in the 12S rRNA (50, 110). Consequently, these mutations render the 28S subunit more susceptible to aminoglycoside binding and inhibition of mitochondrial translation, causing high susceptibility to aminoglycoside-induced ototoxicity in these patients. Even though only 0.2–0.3% of the population harbors these mutations (51–53), up to 20% of patients treated with aminoglycosides for acute bacterial infections may experience irreversible hearing loss (49).

Mechanistic studies of aminoglycoside binding to mutant bacterial ribosomes engineered to contain variants of the mitoribosomal decoding site rRNA have shown that the A1555G and C1494T susceptibility mutations render the ribosome highly susceptible to aminoglycoside binding, leading to miscoding and translation inhibition (110, 111). In the same model system, it was found that the aminoglycoside apramycin showed little toxic effect, even in the presence of the A1555G mutation, possibly because it inserts less deeply into the h44 pocket, which may render its binding more dependent on the presence of the bacterial G1491–C1409 base pair, which is absent even in the mutant mitoribosomal decoding site (**Figure 5*b*,*i***) (112). Apramycin still showed antibacterial activity, indicating that it is possible to design potent but less toxic aminoglycosides (112, 113).

The structures of mammalian mitochondrial and cytosolic ribosomes at near-atomic resolution, in combination with the structures of bacterial ribosomes and cytosolic ribosomes from lower eukaryotes, will facilitate the rational design of compounds that specifically target one type of ribosome without affecting the others, resulting in drugs with improved efficiency and fewer side effects.

mS29, mL41, AND mL65: MITORIBOSOMAL PROTEINS WITH A POSSIBLE ROLE IN APOPTOSIS

Mitochondria are key players in the induction of apoptosis (programmed cell death). The permeabilization of the outer mitochondrial membrane, which is suppressed by the antiapoptotic proteins of the Bcl-2 family and promoted by their proapoptotic antagonists, releases the proteins of the intermembrane space to the cytosol, among them cytochrome *c* (10). Cytochrome *c* is an activator of apoptosome assembly, which triggers downstream apoptotic events by activating effector caspases (114). Interestingly, several mitoribosomal proteins have a role in controlling apoptosis, among them mS29 (death-associated protein 3, DAP3), mL41 (Bcl-2-interacting mitochondrial ribosomal protein, BMRP), and mL65 (programmed cell death 9, PDCD9).

Figure 5

Antibiotic binding to the mitochondrial ribosome. (*a*) A constriction of the yeast mitoribosomal tunnel (*light brown*; PDB identification number 3J6B) sterically interferes with macrolide binding as observed in bacteria (*gold*, erythromycin; PDB identification number 3OHJ). (*b*,*c*) The overall rRNA structure at the tunnel entrance of mammalian mitoribosomes (*light blue*) is similar to that of bacterial rRNA (*light yellow*). Macrolide resistance is conferred by the presence of G1051 (*orange*) instead of bacterial A2058 (*white*). (*d*,*e*) Aminoglycoside antibiotics bind to a pocket (*arrowhead*) near the ribosomal A-site (anticodon stems of A- and P-site tRNA are shown in *yellow* and *purple*; mRNA shown in *red*; PDB identification number 5AJ4). (*f*) Secondary structure of the SSU rRNA near this aminoglycoside-binding pocket in bacteria, mammalian mitochondria, and human mitochondria in the presence and absence of sensitizing mutations (110). (*g*) Structure of the bacterial 30S subunit with bound paromomycin (*cyan*; PDB identification number 2WDK). (*h*) Structure of the mammalian mitoribosomal subunit. Sequence differences leading to the disruption of base pairs are indicated. (*i*) Superposition of the bacterial and mitoribosomal structures. The binding of apramycin (*red*; PDB identification number 4AQY) may depend on the presence of the bacterial C1409–G1491 base pair (*light orange*), which is disrupted in mitoribosomes (C853 and C917, *orange*). Abbreviations: mRNA, messenger RNA; PDB, Protein Data Bank; rRNA, ribosomal RNA; SSU, small subunit; tRNA, transfer RNA.

The mS29 protein was initially identified as a protein involved in interferon-γ-mediated cell death (115). However, the mechanism by which mS29 contributes to apoptotic signaling has been controversial, and it has even been suggested that mS29 does not have an apoptotic function at all (116). Several studies have suggested that mS29 acts in the extrinsic apoptotic pathway, downstream of receptors for extracellular signaling (death receptors) but upstream of caspases (117, 118). However, conflicting evidence has suggested that mS29 functions in the intrinsic (mitochondrial) apoptotic pathway and retains its mitochondrial localization during the induction of apoptosis and mitochondrial fragmentation (119–122).

In the context of the mitoribosome, mS29 associates with the 28S subunit head, where it is involved in extensive contacts with surrounding mitoribosomal proteins, the 12S rRNA, and with intersubunit bridges (**Figure 6*a*,*b***) (62, 63). The mS29 protein confers guanine

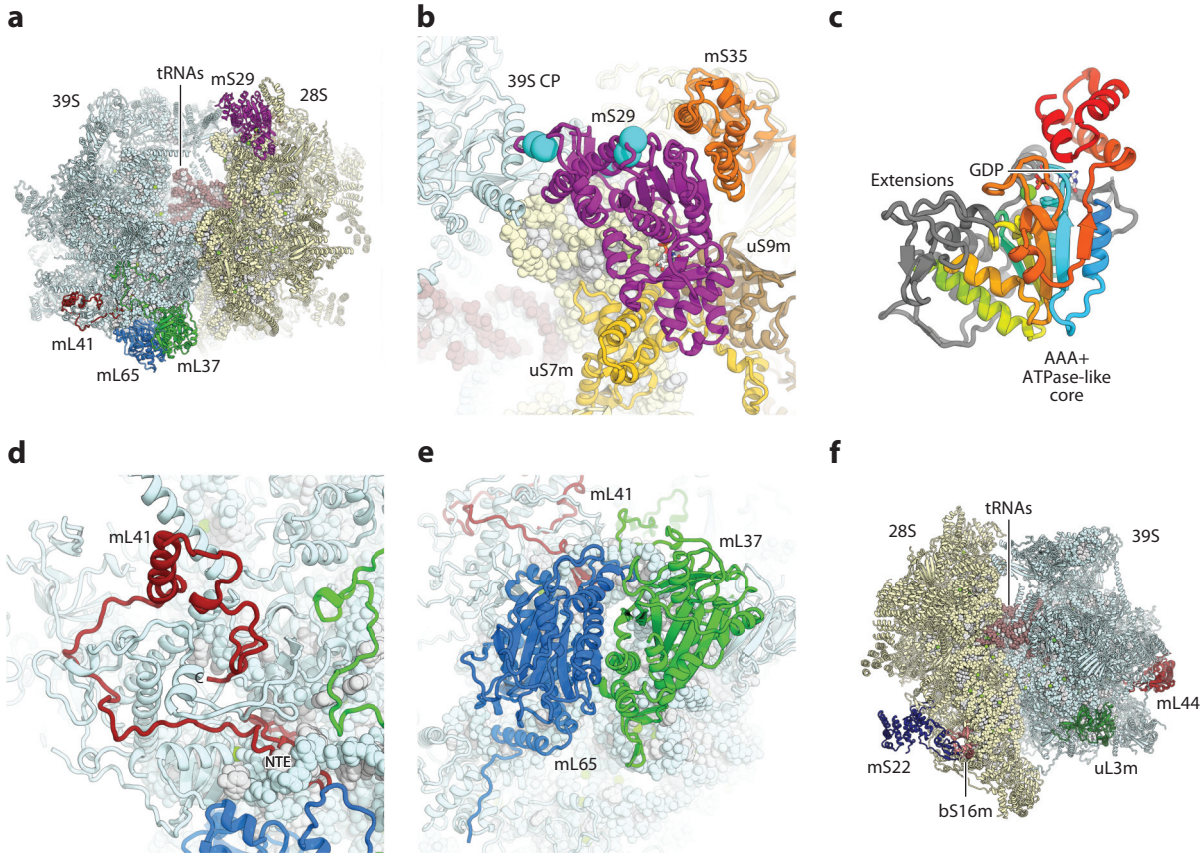

Figure 6

Mitoribosomal proteins involved in apoptosis and human pathologies. (*a*) Overview of the localizations of mS29 (*purple*), mL41 (*red*), and the mL37–mL65 dimer (*green* and *blue*) on the 55S mitoribosome. (*b*) Interactions of mS29 (DAP3) with uS7m (*gold*), uS9m (*brown*), and mS35 (*orange*) of the 28S subunit and the formation of intersubunit bridges to the 39S subunit CP. Phosphorylation sites are indicated as cyan spheres. (*c*) mS29 (DAP3) harbors an AAA+ ATPase-like core fold (shown using a color gradient from *blue* to *red*). (*d*) Structure of mL41. The NTE is deeply embedded within the ribosomal core. (*e*) Structure of the pseudosymmetric mL37–mL65 dimer. (*f*) Mutations in the mitoribosomal proteins mL44 (*red*), uL3m (*green*), bS16m (*pink*), and mS22 (*dark blue*) have been implicated in human pathologies. Abbreviations: ATPase, adenosine triphosphatase; CP, central protuberance; GDP, guanosine diphosphate; NTE, N-terminal extension; tRNA, transfer RNA.

nucleotide-binding activity to the mitochondrial ribosome (123, 124), which is an unusual feature not found in bacterial or eukaryotic cytosolic ribosomes, in which only ribosome-associated initiation and translation factors exhibit GTPase activity. In spite of its specificity for guanine nucleotides, the overall fold of mS29 identifies the protein as a member of the AAA+ ATPase family (**Figure 6*c***) (62, 125). It contains both Walker A and Walker B motifs, conserved sequence motifs typical of AAA+ ATPases and other nucleotide hydrolases (125–127), and is likely to be catalytically active (63). Interestingly, mS29 lacks one of two conserved acidic residues usually found at the end of the Walker B motif (125, 127). This is typical for the NACHT NTPases (nucleoside triphosphatases), a subfamily of the STAND class of AAA+ proteins, in which the preference for guanine nucleotides has been observed before (128). Notably, many STAND NTPases have been implicated in apoptotic regulation in metazoan cells (128).

Both structures of mammalian 55S mitoribosomes show mS29 in the guanosine diphosphate (GDP)-bound form. It appears that the accommodation of a GTP molecule is incompatible with the conformation of mS29 observed in these structures, indicating that GTP binding in the context of the 55S mitoribosome would require structural rearrangements (62, 63). Because 28S subunits bind GTP with higher affinity than they do 55S monosomes (123, 129), nucleotide hydrolysis by mS29 may be coupled to subunit association and the formation of 55S mitoribosomes (63). In addition to its putative regulation by nucleotide binding, mS29 contains several phosphorylation sites (130, 131), which are located close to the regions of the protein involved in the formation of intersubunit bridges (**Figure 6*b***) (62). Therefore, mS29 may function in the regulation of mitochondrial translation and mitoribosomal subunit association, depending on its nucleotide state and phosphorylation status. It remains to be determined whether these activities are coupled to a role of the protein in apoptosis.

The protein mL41 suppresses cell growth by induction of apoptosis and cell cycle arrest (132). Bcl-2 proteins interact directly with mL41 (133) as a means of attenuating its apoptotic activity (134). In the structure of the 39S subunit, mL41 assumes a mostly extended conformation (**Figure 6*d***) (60). It forms tight interactions with many surrounding mitoribosomal proteins, as well as with the 16S rRNA, and it is unlikely to be easily dissociated from the ribosomal particle. The putative Bcl-2 interaction sites near the mL41 N terminus (134) either are buried in the 16S rRNA and are, therefore, inaccessible in the conformation observed in our structure or are missing in the mature protein due to cleavage of the mitochondrial targeting sequence. Therefore, binding to Bcl-2 and any apoptotic activity of mL41 likely take place in the cytosol (134) rather than after mitochondrial import and incorporation into the mitoribosome.

Initially, mL65 was identified as a 28S subunit protein, but the structures of the 39S subunit at near-atomic resolution revealed it to be a large subunit protein that forms a pseudosymmetric heterodimer with the homologous protein mL37 (**Figure 6*e***) (60, 61). The chicken homolog of mL65, termed p52, can induce apoptosis in mammalian culture cells upon overexpression (135), and mL65 has been found to be upregulated in estrogen-receptor-positive breast cancer cells (136). The molecular mechanisms of mL65 activity in these roles remain to be established as does whether they involve the ribosome-bound form of the protein.

The presence of several apoptosis-controlling proteins on the mammalian mitoribosome has led to the idea that mitochondrial translation, or the mitoribosome itself, might be involved in apoptotic signaling (15, 124). However, for cytosolic ribosomal proteins it has been well established that many of them also perform extraribosomal functions (137), and this might apply also to mitoribosomal proteins. In the light of the most recent structural data demonstrating the tight association of mS29, mL41, and mL65 with the rest of the 55S mitoribosome, these mitoribosomal proteins may perform their apoptotic functions away from the ribosome in an extraribosomal pool, with the possible exception of mS29, which might be a candidate for controlling mitochondrial translation.

THE MITORIBOSOME IN HUMAN PATHOLOGIES

In addition to the involvement of the mitoribosome in aminoglycoside-induced ototoxicity (see section on Binding of Antibiotics to Mitoribosomes), mutations in components of the mitochondrial ribosome are associated with hereditary diseases. Respiratory-chain disorders represent a diverse range of diseases and occur with a prevalence of roughly 1 in 5,000–7,500 live births (39, 138). A subset of these disorders is caused by defects in mitochondrial translation and can arise from mutations in most components of the mitochondrial translation machinery, including tRNAs, aminoacyl-tRNA synthetases, translation factors, and ribosomal components (39, 139). Documented cases with mutations in ribosomal proteins include mutations in uL3m (43), uL12m (140), mL44 (41), mS22 (42, 44), bS16m (45), and uS7m (141) (**Figure 6*f***). These mutations commonly cause instability of the protein, impaired assembly of the affected mitoribosomal subunit (41, 142), a deficiency in oxidative phosphorylation, and a variety of severe phenotypes, including dysmorphism, lactic acidosis, neurological disorders, and cardiomyopathies, which are often fatal early in life. Although these protein mutations hamper the biogenesis of their corresponding ribosomal subunit, the other subunit usually remains unaffected, indicating that mitoribosomal subunits are assembled and matured largely independently of each other (41, 142). The occurrence of dysmorphism in patients with affected mitoribosomal small-subunit biogenesis hints at a function of this subunit in fetal development in addition to respiratory-chain function (41, 42, 45).

Because a number of mitoribosomal proteins are involved in apoptotic signaling and the regulation of cell proliferation, their altered expression has been associated with the development of cancer (see section on mS29, mL41, and mL65: Mitoribosomal Proteins with a Possible Role in Apoptosis). Additionally, elevated mitochondrial translation may be needed to provide the metabolic capacity to meet the energy requirements of cancer cells. Even though ATP production in cancer cells has long been thought to occur mostly by glycolysis in the cytoplasm (143), recent evidence has indicated that some types of cancer cells may rely heavily on oxidative phosphorylation in their mitochondria, utilizing metabolites provided by neighboring glycolytic stromal cells (144) or by cancer cells in more poorly oxygenated regions of the cancer (145). In agreement with these ideas, the upregulation of a large number of mitoribosomal proteins has been observed in human breast cancer cells, but not in adjacent stromal cells, leading to the proposal that mitochondria fuel epithelial cancer cell metabolism (46). Therefore, it has been proposed that targeting mitochondrial translation may be a promising strategy for cancer therapy (146). Interfering with mitochondrial translation by treatment with tigecycline or the knock down of mitochondrial EF-Tu selectively inhibits the proliferation of leukemia cells, suggesting that tigecycline may possibly be an anticancer agent (48, 147).

The inhibition of mitochondrial peptide deformylase, the enzyme that removes the formyl group from initiator methionines (148), by actinonin antibiotics inhibits the growth of several human cancer cell lines (149). The antiproliferative effect of peptide deformylase inhibition has been attributed to a signaling response elicited by the presence of stalled mitoribosomes and the resultant activation of an RNA decay pathway, explaining why the inhibition of mitochondrial protein synthesis also affects cancer cells that depend on glycolysis in the cytoplasm for their metabolism (47, 143).

INSIGHTS INTO MITORIBOSOME EVOLUTION: COMPARISON OF THE MAMMALIAN 39S AND YEAST 54S MITORIBOSOMAL LARGE SUBUNITS

As discussed above, several important differences exist between the mammalian 39S and yeast 54S large mitoribosomal subunits: (*a*) Although both mitoribosomal subunits share a common set

of mitochondrial-specific proteins, they also contain proteins specific to their respective lineages (**Figure 7*a–f***). (*b*) The 54S subunit contains numerous rRNA expansion segments, but the 39S subunit rRNA is strongly reduced (**Figure 7*g–l***). (*c*) The 54S subunit does not contain an equivalent to the 5S rRNA or CP tRNA (**Figure 3**) (57). (*d*) The path of the mitoribosomal tunnel differs between the 54S and 39S subunits (**Figure 2**) (56, 57, 60, 61). The analysis of these differences and the comparison of the mitoribosomal large subunits to the bacterial 50S subunit can aid our understanding of the evolution of the mitoribosome (**Figure 8*a***).

Analyses of the interactions of two mitoribosomal proteins with homology to RNA-binding proteins, the threonyl-tRNA synthetase homolog mL39 (150) and the RNase III homolog mL44 (17), have suggested that their initial recruitment to the mitoribosome occurred via interactions with rRNA elements (**Figure 8*b***) (57, 60). The formation of clusters of rRNA expansion segments and the recruitment of specific ribosomal proteins to them have also been observed in the eukaryotic cytosolic ribosome (72, 73), and these developments may be general features of expansive ribosome evolution. Due to their stable incorporation into the ribosomal subunit by subsequently evolved protein–protein contacts, both mL39 and mL44 have been retained in the mammalian mitoribosome even though their initial interactions with rRNA were lost during rRNA reduction (**Figure 8*c***) (60). These observations strongly suggest that the presence of expansion segments was a universal feature during early mitoribosomal evolution rather than a specialty of the yeast mitoribosome and that the strong reduction of rRNA is a feature specific to a few taxonomic groups, such as metazoans and intracellular parasites. These evolutionary trends can be understood in the context of a recently proposed framework that postulates two major phases of mitoribosome evolution (25): first, a constructive phase, during which new mitoribosomal proteins were recruited and the rRNAs expanded (**Figure 9*a*,*b***), and, second, a destructive phase specific to a few lineages, including mammals, during which the rRNAs were dramatically reduced in length and the recruitment of additional proteins continued (**Figure 9*c***) (25). Both phases were driven by the accumulation of slightly deleterious mutations in mitochondrial-encoded rRNA components of the mitoribosome (25).

The polypeptide tunnel paths in mammalian mitoribosomes and bacterial ribosomes are similar to each other (60, 61) (**Figure 2*a*,*b***). The yeast mitoribosome, however, exhibits two major differences to its counterpart in bacterial ribosomes. Close to the PTC, an alteration in the rRNA structure forming the tunnel wall leads to a constriction not present in bacterial ribosomes (**Figure 5*a***), which may alter some antibiotic-binding sites in the tunnel (see section on Binding of Antibiotics to Mitoribosomes) (57). Additionally, the exit in the yeast mitoribosomal tunnel is shifted relative to the bacterial exit site because of an extension of uL23 that partially blocks the canonical path of the nascent chain, but an rRNA deletion opens an alternative exit site (**Figure 2*c***) (57). Current structural data suggest that the bacterial YidC membrane protein insertase—a homolog of the mitochondrial Oxa1 insertase—binds close to the exit of the bacterial polypeptide tunnel (151, 152). Therefore, the nascent chain may need to be routed to the insertase complex across the ribosomal subunit surface due to the relocation of the polypeptide tunnel exit in the 54S yeast large subunit (57). Alternatively, the binding site of the insertase on the 54S subunit would have to be relocated together with the tunnel exit. However, cryo-EM tomographic data for membrane-bound yeast mitoribosomes have suggested that this is less likely (**Figure 4*i***) (32). Higher-resolution structural data of the mammalian and yeast mitoribosome–Oxa1 complexes are required to ensure a detailed understanding of the mechanism and evolution of membrane protein insertion in mitochondria.

In summary, these observations suggest that after the endosymbiotic event at the origin of mitochondria, a mitoribosome evolved that (*a*) had incorporated a number of mitochondrial-specific proteins into its structure, (*b*) contained expansion segments in its rRNA, and (*c*) featured a bacterial-like polypeptide exit-tunnel path (**Figure 8**). After the divergence of the eukaryotic

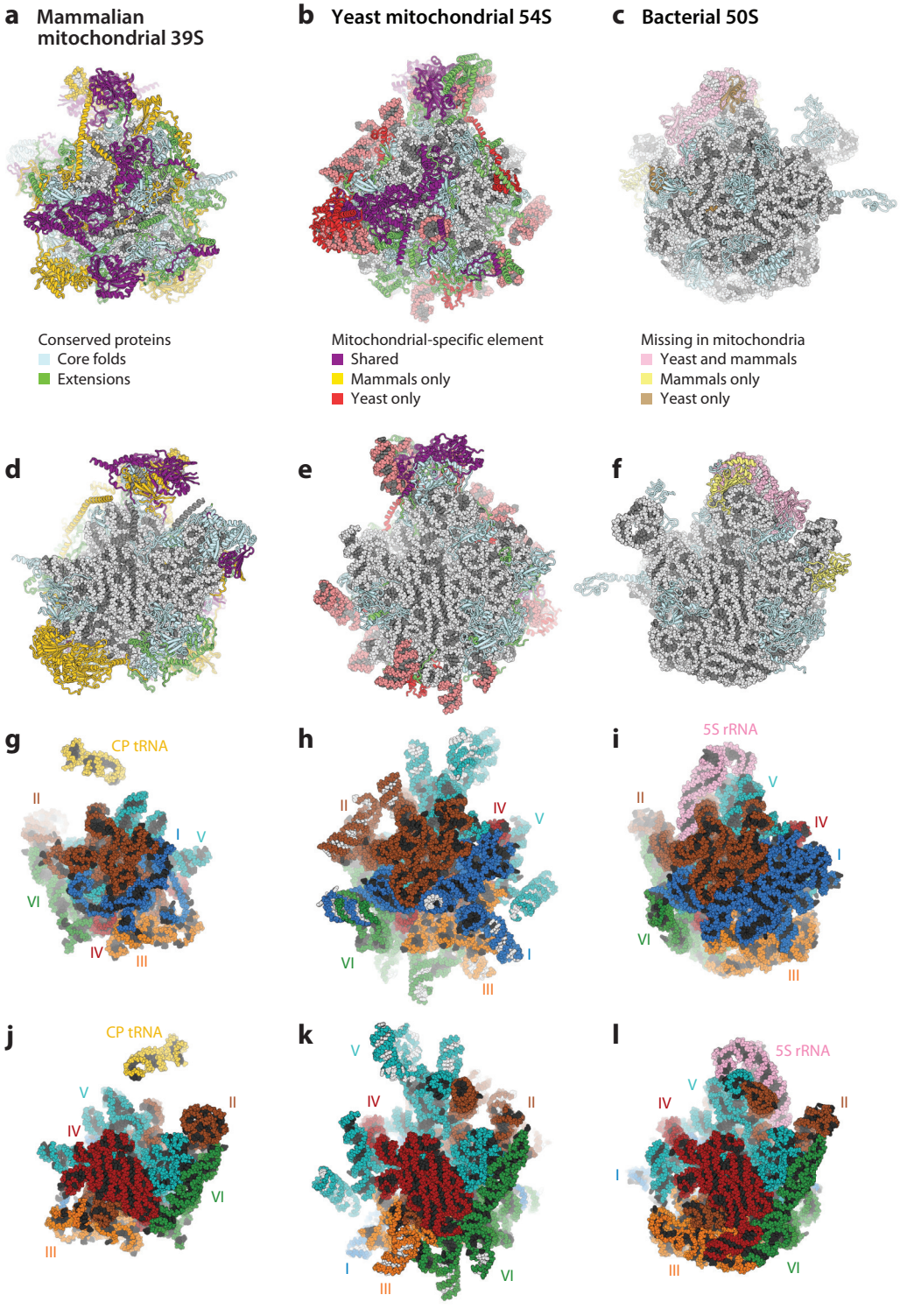
a
Mammalian mitochondrial 39S
b
Yeast mitochondrial 54S
c
Bacterial 50S
Conserved proteins
Core folds
Extensions
Mitochondrial-specific element
Shared
Mammals only
Yeast only
Missing in mitochondria
Yeast and mammals
Mammals only
Yeast only
d
e
f
g
CP tRNA
II
I
V
VI
IV
III
h
II
IV
V
VI
I
III
i
5S rRNA
V
II
IV
I
VI
III
j
CP tRNA
V
II
IV
VI
III
k
V
IV
II
I
III
VI
l
5S rRNA
V
IV
II
I
III
VI

Figure 7

Comparison of the bacterial, yeast mitochondrial, and mammalian mitochondrial ribosomal large subunits. (*a–f*) Mammalian 39S (*left*; PDB identification number 5AJ4), yeast 54S (*middle*; PDB identification number 3J6B), and bacterial 50S (*right*; PDB identification number 4V5D) subunits shown in (*a–c*) solvent-side and (*d–f*) subunit-interface views. Conserved proteins are shown in light blue, with extensions of these proteins in green. Mitochondrial-specific proteins occurring in lower and higher eukaryotes are shown in purple. Proteins and rRNA elements (CP tRNA and expansion segments) specific to mammals are shown in gold, those specific to yeast in red, and those specific to bacteria in light pink. (*g–l*) Comparison of large subunit rRNA structures (views as in *a–f*). CP tRNA is shown in gold and 5S rRNA in light pink. 16S, 21S, and 23S rRNA are color coded by domain (*blue*, domain I; *brown*, domain II; *orange*, domain III; *red*, domain IV; *cyan*, domain V; *green*, domain VI). Nucleotide bases are shown in black, except for the expansion segments of the yeast mitochondrial 21S rRNA, where they are shown in white. Abbreviations: CP, central protuberance; PDB, Protein Data Bank; rRNA, ribosomal RNA; tRNA, transfer RNA.

lineages, protein recruitment to the mitoribosome continued in both the fungal and metazoan lines. The yeast mitoribosome retained the rRNA expansion segments and acquired an altered polypeptide tunnel, with modifications to both the tunnel entry and exit. In contrast, in the lineage leading to mammals, the rRNA was strongly reduced while the basic tunnel geometry was maintained. The sequence of events leading to the acquisition of the CP tRNA in the mammalian lineage is more difficult to reconstruct. Because the yeast 54S subunit lacks both the CP tRNA and uL18m, it is likely that the common ancestral mitoribosome contained an RNA molecule in the CP that interacted with uL18m, both of which were lost and partially replaced by an expansion segment in the yeast lineage (**Figure 8*a***).

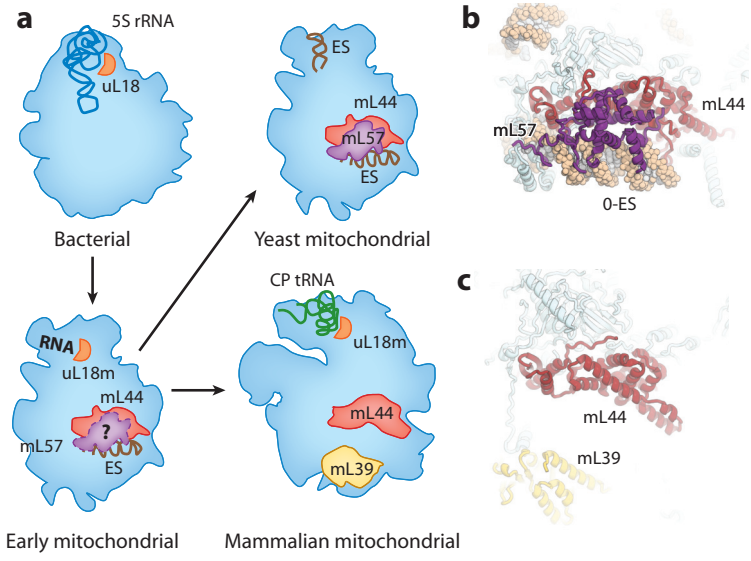

Figure 8

Molecular evolution of the mitoribosome. (*a*) Schematic of the series of events leading to the acquisition of mL39, mL44, and mL57, and the reorganization of the mitoribosomal CP. (*b*,*c*) Detailed views of the region around mL44. (*b*) Yeast mitoribosomes harbor an rRNA ES in the vicinity of where mL44 and mL57 have been recruited. (*c*) Mammalian mitoribosomes still contain mL44, but have lost the ES and mL57. Abbreviations: CP, central protuberance; ES, expansion segment; rRNA, ribosomal RNA.

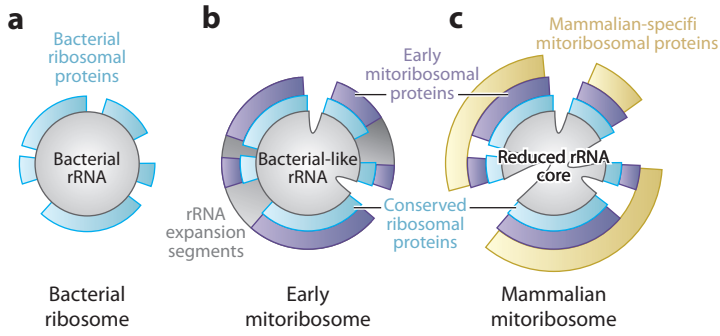

Figure 9

Schematic of the two major phases of mitoribosomal evolution. From the bacterial ribosome (*a*), early mitoribosomes (*b*) evolved by adding rRNA ESs and specific mitoribosomal proteins. Mammalian mitoribosomes (*c*) lost their rRNA expansion segments, their rRNA was reduced to an innermost core, and additional mitoribosomal proteins were acquired on their surface. Abbreviations: ES, expansion segment; rRNA, ribosomal RNA.

SUMMARY POINTS

1. The structures have been determined at near-atomic resolution of empty, as well as transfer RNA (tRNA)- and messenger RNA (mRNA)-containing, mammalian mitoribosomes and the yeast mitoribosomal large subunit.
2. These structures have allowed for the building of near-complete models of the mitoribosomal RNAs and the determination of the locations and folds of all mammalian mitoribosomal proteins.
3. The structures have provided insight into unique features of the mitoribosome, including the recruitment of mRNAs, the presence of a unique architectural tRNA in the central protuberance in some organisms, the altered and variable structure of the polypeptide exit tunnel, and the mechanism of membrane attachment of mitoribosomes.
4. We introduce here a unified nomenclature for mitoribosomal proteins and intersubunit bridges based on the naming proposed in structural work published in late 2014 and early 2015.

FUTURE ISSUES

1. Structural studies of the mitoribosomal translation-initiation pathway are required to gain further insight into mRNA recruitment and start codon selection in mitochondria.
2. Structural analyses of the mitoribosome bound to the associated membrane protein insertase complexes will reveal the specialized mechanics of membrane protein insertion in mitochondria.
3. Higher-resolution determination of the structures of mammalian mitoribosomes bound to antibiotics or inhibitors will facilitate the development of more specific inhibitors to be used as antibiotics or anticancer compounds.

4. Analyses of the full range of mitoribosomal motions should be undertaken using an in vitro tRNA translocation reaction.
5. Determining the complete structure of the yeast mitoribosome and structures of mitoribosomes from pathogenic organisms will provide insights into the evolution and diversity of mitochondrial ribosomes and may facilitate the development of compounds interfering with mitochondrial translation in these organisms.

DISCLOSURE STATEMENT

The authors are not aware of any affiliations, memberships, funding, or financial holdings that might be perceived as affecting the objectivity of this review.

ACKNOWLEDGMENTS

The authors thank Venki Ramakrishnan, Alexey Amunts, Alan Brown, Daniel Boehringer, Philipp Bieri, and Marc Leibundgut for discussions. The representations of the molecular structures were created using UCSF Chimera (**http://www.cgl.ucsf.edu/chimera/**) (153) and PyMOL (The PyMOL Molecular Graphics System, version 1.7, Schrödinger LLC, **https://www.pymol.org/**). This work was supported by the Swiss National Science Foundation (SNSF) and the National Centers of Excellence in Research (NCCR) RNA & Disease program of the SNSF. B.J.G. was supported by an Advanced Postdoc Mobility fellowship from the SNSF (project 160983).

LITERATURE CITED

1. Schmeing TM, Ramakrishnan V. 2009. What recent ribosome structures have revealed about the mechanism of translation. *Nature* 461:1234–42
2. Steitz TA. 2008. A structural understanding of the dynamic ribosome machine. *Nat. Rev. Mol. Cell Biol.* 9:242–53
3. Ogle JM, Brodersen DE, Clemons WM, Tarry MJ, Carter AP, Ramakrishnan V. 2001. Recognition of cognate transfer RNA by the 30S ribosomal subunit. *Science* 292:897–902
4. Nissen P, Hansen J, Ban N, Moore PB, Steitz TA. 2000. The structural basis of ribosome activity in peptide bond synthesis. *Science* 289:920–30
5. Ban N, Nissen P, Hansen J, Moore PB, Steitz TA. 2000. The complete atomic structure of the large ribosomal subunit at 2.4 Å resolution. *Science* 289:905–20
6. Polikanov YS, Steitz TA, Innis CA. 2014. A proton wire to couple aminoacyl-tRNA accommodation and peptide-bond formation on the ribosome. *Nat. Struct. Mol. Biol.* 21:787–93
7. Beringer M, Rodnina MV. 2007. The ribosomal peptidyl transferase. *Mol. Cell* 26:311–21
8. Jenni S, Ban N. 2003. The chemistry of protein synthesis and voyage through the ribosomal tunnel. *Curr. Opin. Struct. Biol.* 13:212–19
9. Kramer G, Boehringer D, Ban N, Bukau B. 2009. The ribosome as a platform for co-translational processing, folding and targeting of newly synthesized proteins. *Nat. Struct. Mol. Biol.* 16:589–97
10. Tait SWG, Green DR. 2010. Mitochondria and cell death: outer membrane permeabilization and beyond. *Nat. Rev. Mol. Cell Biol.* 11:621–32
11. López-Otín C, Blasco MA, Partridge L, Serrano M, Kroemer G. 2013. The hallmarks of aging. *Cell* 153:1194–217
12. Sagan L. 1967. On the origin of mitosing cells. *J. Theor. Biol.* 14:255–74
13. Andersson SG, Zomorodipour A, Andersson JO, Sicheritz-Pontén T, Alsmark UC, et al. 1998. The genome sequence of *Rickettsia prowazekii* and the origin of mitochondria. *Nature* 396:133–40

14. O'Brien TW. 2002. Evolution of a protein-rich mitochondrial ribosome: implications for human genetic disease. *Gene* 286:73–79

15. The first cryo-EM reconstruction of a mitoribosome revealed its unique overall morphology.

15. Sharma MR, Koc EC, Datta PP, Booth TM, Spremulli LL, Agrawal RK. 2003. Structure of the mammalian mitochondrial ribosome reveals an expanded functional role for its component proteins. *Cell* 115:97–108

16. Koc EC, Cimen H, Kumcuoglu B, Abu N, Akpinar G, et al. 2013. Identification and characterization of CHCHD1, AURKAIP1, and CRIF1 as new members of the mammalian mitochondrial ribosome. *Front. Physiol.* 4:183
17. Koc EC, Burkhart W, Blackburn K, Moyer MB, Schlatzer DM, et al. 2001. The large subunit of the mammalian mitochondrial ribosome: analysis of the complement of ribosomal proteins present. *J. Biol. Chem.* 276:43958–69
18. Koc EC, Burkhart W, Blackburn K, Moseley A, Spremulli LL. 2001. The small subunit of the mammalian mitochondrial ribosome. Identification of the full complement of ribosomal proteins present. *J. Biol. Chem.* 276:19363–74
19. Suzuki T, Terasaki M, Takemoto-Hori C, Hanada T, Ueda T, et al. 2001. Structural compensation for the deficit of rRNA with proteins in the mammalian mitochondrial ribosome: systematic analysis of protein components of the large ribosomal subunit from mammalian mitochondria. *J. Biol. Chem.* 276:21724–36
20. Suzuki T, Terasaki M, Takemoto-Hori C, Hanada T, Ueda T, et al. 2001. Proteomic analysis of the mammalian mitochondrial ribosome: identification of protein components in the 28 S small subunit. *J. Biol. Chem.* 276:33181–95
21. Desmond E, Brochier-Armanet C, Forterre P, Gribaldo S. 2011. On the last common ancestor and early evolution of eukaryotes: reconstructing the history of mitochondrial ribosomes. *Res. Microbiol.* 162:53–70
22. Smits P, Smeitink JAM, van den Heuvel LP, Huynen MA, Ettema TJG. 2007. Reconstructing the evolution of the mitochondrial ribosomal proteome. *Nucleic Acids Res.* 35:4686–703
23. Stegeman WJ, Cooper CS, Avers CJ. 1970. Physical characterization of ribosomes from purified mitochondria of yeast. *Biochem. Biophys. Res. Commun.* 39:69–76
24. Küntzel H, Noll H. 1967. Mitochondrial and cytoplasmic polysomes from *Neurospora crassa*. *Nature* 215:1340–45

25. Analyzed the molecular evolution of the mitoribosome and the complexes of the mitochondrial respiratory chain.

25. van der Sluis EO, Bauerschmitt H, Becker T, Mielke T, Frauenfeld J, et al. 2015. Parallel structural evolution of mitochondrial ribosomes and OXPHOS complexes. *Genome Biol. Evol.* 7:1235–51

26. Attardi G, Ojala D. 1971. Mitochondrial ribosome in HeLa cells. *Nat. New Biol.* 229:133–36
27. Anderson S, Bankier AT, Barrell BG, de Bruijn MH, Coulson AR, et al. 1981. Sequence and organization of the human mitochondrial genome. *Nature* 290:457–65
28. Eperon IC, Janssen JW, Hoeijmakers JH, Borst P. 1983. The major transcripts of the kinetoplast DNA of *Trypanosoma brucei* are very small ribosomal RNAs. *Nucleic Acids Res.* 11:105–25
29. Ott M, Herrmann JM. 2010. Co-translational membrane insertion of mitochondrially encoded proteins. *Biochim. Biophys. Acta* 1803:767–75
30. Liu M, Spremulli L. 2000. Interaction of mammalian mitochondrial ribosomes with the inner membrane. *J. Biol. Chem.* 275:29400–6
31. Ott M, Prestele M, Bauerschmitt H, Funes S, Bonnefoy N, Herrmann JM. 2006. Mba1, a membrane-associated ribosome receptor in mitochondria. *EMBO J.* 25:1603–10

32. Presented cryo-EM tomography of the yeast mitoribosome attached to the mitochondrial inner membrane.

32. Pfeffer S, Woellhaf MW, Herrmann JM, Förster F. 2015. Organization of the mitochondrial translation machinery studied in situ by cryoelectron tomography. *Nat. Commun.* 6:6019

33. Jones CN, Wilkinson KA, Hung KT, Weeks KM, Spremulli LL. 2008. Lack of secondary structure characterizes the 5′ ends of mammalian mitochondrial mRNAs. *RNA* 14:862–71
34. Montoya J, Ojala D, Attardi G. 1981. Distinctive features of the 5′-terminal sequences of the human mitochondrial mRNAs. *Nature* 290:465–70
35. Shine J, Dalgarno L. 1974. The 3′-terminal sequence of *Escherichia coli* 16S ribosomal RNA: complementarity to nonsense triplets and ribosome binding sites. *PNAS* 71:1342–46
36. Herrmann JM, Woellhaf MW, Bonnefoy N. 2013. Control of protein synthesis in yeast mitochondria: the concept of translational activators. *Biochim. Biophys. Acta* 1833:286–94

37. Gaur R, Grasso D, Datta PP, Krishna PDV, Das G, et al. 2008. A single mammalian mitochondrial translation initiation factor functionally replaces two bacterial factors. *Mol. Cell* 29:180–90
38. Rötig A. 2011. Human diseases with impaired mitochondrial protein synthesis. *Biochim. Biophys. Acta* 1807:1198–205
39. Vafai SB, Mootha VK. 2012. Mitochondrial disorders as windows into an ancient organelle. *Nature* 491:374–83
40. Pearce S, Nezich CL, Spinazzola A. 2013. Mitochondrial diseases: Translation matters. *Mol. Cell. Neurosci.* 55:1–12
41. Carroll CJ, Isohanni P, Pöyhönen R, Euro L, Richter U, et al. 2013. Whole-exome sequencing identifies a mutation in the mitochondrial ribosome protein MRPL44 to underlie mitochondrial infantile cardiomyopathy. *J. Med. Genet.* 50:151–59
42. Smits P, Saada A, Wortmann SB, Heister AJ, Brink M, et al. 2011. Mutation in mitochondrial ribosomal protein MRPS22 leads to Cornelia de Lange–like phenotype, brain abnormalities and hypertrophic cardiomyopathy. *Eur. J. Hum. Genet.* 19:394–99
43. Galmiche L, Serre V, Beinat M, Assouline Z, Lebre A-S, et al. 2011. Exome sequencing identifies MRPL3 mutation in mitochondrial cardiomyopathy. *Hum. Mutat.* 32:1225–31
44. Saada A, Shaag A, Arnon S, Dolfin T, Miller C, et al. 2007. Antenatal mitochondrial disease caused by mitochondrial ribosomal protein (MRPS22) mutation. *J. Med. Genet.* 44:784–86
45. Miller C, Saada A, Shaul N, Shabtai N, Ben-Shalom E, et al. 2004. Defective mitochondrial translation caused by a ribosomal protein (MRPS16) mutation. *Ann. Neurol.* 56:734–38
46. Sotgia F, Whitaker-Menezes D, Martinez-Outschoorn UE, Salem AF, Tsirigos A, et al. 2012. Mitochondria "fuel" breast cancer metabolism: Fifteen markers of mitochondrial biogenesis label epithelial cancer cells, but are excluded from adjacent stromal cells. *Cell Cycle* 11:4390–401
47. Richter U, Lahtinen T, Marttinen P, Myöhänen M, Greco D, et al. 2013. A mitochondrial ribosomal and RNA decay pathway blocks cell proliferation. *Curr. Biol.* 23:535–41
48. Skrtić M, Sriskanthadevan S, Jhas B, Gebbia M, Wang X, et al. 2011. Inhibition of mitochondrial translation as a therapeutic strategy for human acute myeloid leukemia. *Cancer Cell* 20:674–88
49. Xie J, Talaska AE, Schacht J. 2011. New developments in aminoglycoside therapy and ototoxicity. *Hear. Res.* 281:28–37
50. Prezant TR, Agapian JV, Bohlman MC, Bu X, Oztas S, et al. 1993. Mitochondrial ribosomal RNA mutation associated with both antibiotic-induced and non-syndromic deafness. *Nat. Genet.* 4:289–94
51. Bitner-Glindzicz M, Pembrey M, Duncan A, Heron J, Ring SM, et al. 2009. Prevalence of mitochondrial 1555A–G mutation in European children. *N. Engl. J. Med.* 360:640–42
52. Ealy M, Lynch KA, Meyer NC, Smith RJH. 2011. The prevalence of mitochondrial mutations associated with aminoglycoside-induced sensorineural hearing loss in an NICU population. *Laryngoscope* 121:1184–86
53. Vandebona H, Mitchell P, Manwaring N, Griffiths K, Gopinath B, et al. 2009. Prevalence of mitochondrial 1555A–G mutation in adults of European descent. *N. Engl. J. Med.* 360:642–44
54. Mears JA, Sharma MR, Gutell RR, McCook AS, Richardson PE, et al. 2006. A structural model for the large subunit of the mammalian mitochondrial ribosome. *J. Mol. Biol.* 358:193–212
55. Bai X-C, McMullan G, Scheres SHW. 2015. How cryo-EM is revolutionizing structural biology. *Trends Biochem. Sci.* 40:49–57
56. Greber BJ, Boehringer D, Leitner A, Bieri P, Voigts-Hoffmann F, et al. 2014. Architecture of the large subunit of the mammalian mitochondrial ribosome. *Nature* 505:515–19
57. Amunts A, Brown A, Bai X-C, Llácer JL, Hussain T, et al. 2014. Structure of the yeast mitochondrial large ribosomal subunit. *Science* 343:1485–89
58. Walzthoeni T, Leitner A, Stengel F, Aebersold R. 2013. Mass spectrometry supported determination of protein complex structure. *Curr. Opin. Struct. Biol.* 23:252–60
59. Kaushal PS, Sharma MR, Booth TM, Haque EM, Tung CS, et al. 2014. Cryo-EM structure of the small subunit of the mammalian mitochondrial ribosome. *PNAS* 111:7284–89
60. Greber BJ, Boehringer D, Leibundgut M, Bieri P, Leitner A, et al. 2014. The complete structure of the large subunit of the mammalian mitochondrial ribosome. *Nature* 515:283–86

56. Cryo-EM structure and CX–MS data provided insights into the membrane attachment of the mammalian 39S subunit.

57. Presented the fully refined atomic structure of the yeast 54S mitoribosomal subunit as determined by cryo-EM.

60. Identified the CP tRNA in the 3.4 Å resolution of the structure of the porcine 39S subunit.

61. Brown A, Amunts A, Bai X-C, Sugimoto Y, Edwards PC, et al. 2014. Structure of the large ribosomal subunit from human mitochondria. *Science* 346:718–22

62. Greber BJ, Bieri P, Leibundgut M, Leitner A, Aebersold R, et al. 2015. The complete structure of the 55S mammalian mitochondrial ribosome. *Science* 348:303–8

63. Amunts A, Brown A, Toots J, Scheres SHW, Ramakrishnan V. 2015. The structure of the human mitochondrial ribosome. *Science* 348:95–98

64. Ban N, Beckmann R, Cate JHD, Dinman JD, Dragon F, et al. 2014. A new system for naming ribosomal proteins. *Curr. Opin. Struct. Biol.* 24:165–69

65. Yusupov MM, Yusupova GZ, Baucom A, Lieberman K, Earnest TN, et al. 2001. Crystal structure of the ribosome at 5.5 Å resolution. *Science* 292:883–96

66. Dunkle JA, Wang L, Feldman MB, Pulk A, Chen VB, et al. 2011. Structures of the bacterial ribosome in classical and hybrid states of tRNA binding. *Science* 332:981–84

67. Frank J, Agrawal RK. 2000. A ratchet-like inter-subunit reorganization of the ribosome during translocation. *Nature* 406:318–22

68. Budkevich TV, Giesebrecht J, Behrmann E, Loerke J, Ramrath DJF, et al. 2014. Regulation of the mammalian elongation cycle by subunit rolling: a eukaryotic-specific ribosome rearrangement. *Cell* 158:121–31

69. O'Brien TW. 2003. Properties of human mitochondrial ribosomes. *IUBMB Life* 55:505–13

70. Fischmann OT, Hruza A, Niu XD, Fossetta JD, Lunn CA, et al. 1999. Structural characterization of nitric oxide synthase isoforms reveals striking active-site conservation. *Nat. Struct. Biol.* 6:233–42

71. Voorhees RM, Weixlbaumer A, Loakes D, Kelley AC, Ramakrishnan V. 2009. Insights into substrate stabilization from snapshots of the peptidyl transferase center of the intact 70S ribosome. *Nat. Struct. Mol. Biol.* 16:528–33

72. Klinge S, Voigts-Hoffmann F, Leibundgut M, Arpagaus S, Ban N. 2011. Crystal structure of the eukaryotic 60S ribosomal subunit in complex with initiation factor 6. *Science* 334:941–48

73. Ben-Shem A, Garreau de Loubresse N, Melnikov S, Jenner L, Yusupova G, Yusupov M. 2011. The structure of the eukaryotic ribosome at 3.0 Å resolution. *Science* 334:1524–29

74. Smirnov A, Entelis N, Martin RP, Tarassov I. 2011. Biological significance of 5S rRNA import into human mitochondria: role of ribosomal protein MRP-L18. *Genes Dev.* 25:1289–305

75. Yoshionari S, Koike T, Yokogawa T, Nishikawa K, Ueda T, et al. 1994. Existence of nuclear-encoded 5S-rRNA in bovine mitochondria. *FEBS Lett.* 338:137–42

76. Magalhães PJ, Andreu AL, Schon EA. 1998. Evidence for the presence of 5S rRNA in mammalian mitochondria. *Mol. Biol. Cell* 9:2375–82

77. Montoya J, Gaines GL, Attardi G. 1983. The pattern of transcription of the human mitochondrial rRNA genes reveals two overlapping transcription units. *Cell* 34:151–59

78. Helm M, Brulé H, Friede D, Giegé R, Pütz D, Florentz C. 2000. Search for characteristic structural features of mammalian mitochondrial tRNAs. *RNA* 6:1356–79

79. Agrawal RK, Sharma MR. 2012. Structural aspects of mitochondrial translational apparatus. *Curr. Opin. Struct. Biol.* 22:797–803

80. Nierhaus KH. 2006. Decoding errors and the involvement of the E-site. *Biochimie* 88:1013–19

81. Wilson DN, Nierhaus KH. 2006. The E-site story: the importance of maintaining two tRNAs on the ribosome during protein synthesis. *Cell. Mol. Life Sci.* 63:2725–37

82. Koch M, Clementi N, Rusca N, Vögele P, Erlacher M, Polacek N. 2015. The integrity of the G2421-C2395 base pair in the ribosomal E-site is crucial for protein synthesis. *RNA Biol.* 12:70–81

83. Kaushal PS, Sharma MR, Agrawal RK. 2015. The 55S mammalian mitochondrial ribosome and its tRNA-exit region. *Biochimie* 114:119–26

84. Takyar S, Hickerson RP, Noller HF. 2005. mRNA helicase activity of the ribosome. *Cell* 120:49–58

85. Filipovska A, Rackham O. 2013. Pentatricopeptide repeats: modular blocks for building RNA-binding proteins. *RNA Biol.* 10:1426–32

86. Yin P, Li Q, Yan C, Liu Y, Liu J, et al. 2013. Structural basis for the modular recognition of single-stranded RNA by PPR proteins. *Nature* 504:168–71

61. Identified the CP tRNA in the 3.4 Å resolution of the structure of the human 39S subunit.

62. Revealed the complete structure of the porcine 55S mitoribosome in complex with mRNA and tRNA.

63. Revealed the structure of the human 55S mitoribosome using cryo-EM.

87. Davies SMK, Rackham O, Shearwood A-MJ, Hamilton KL, Narsai R, et al. 2009. Pentatricopeptide repeat domain protein 3 associates with the mitochondrial small ribosomal subunit and regulates translation. *FEBS Lett.* 583:1853–58
88. Koc EC, Spremulli LL. 2003. RNA-binding proteins of mammalian mitochondria. *Mitochondrion* 2:277–91
89. Laurberg M, Asahara H, Korostelev A, Zhu J, Trakhanov S, Noller HF. 2008. Structural basis for translation termination on the 70S ribosome. *Nature* 454:852–57
90. Weixlbaumer A, Jin H, Neubauer C, Voorhees RM, Petry S, et al. 2008. Insights into translational termination from the structure of RF2 bound to the ribosome. *Science* 322:953–56
91. Temperley R, Richter R, Dennerlein S, Lightowlers RN, Chrzanowska-Lightowlers ZM. 2010. Hungry codons promote frameshifting in human mitochondrial ribosomes. *Science* 327:301
92. Richter R, Rorbach J, Pajak A, Smith PM, Wessels HJ, et al. 2010. A functional peptidyl-tRNA hydrolase, ICT1, has been recruited into the human mitochondrial ribosome. *EMBO J.* 29:1116–25
93. Akabane S, Ueda T, Nierhaus KH, Takeuchi N. 2014. Ribosome rescue and translation termination at non-standard stop codons by ICT1 in mammalian mitochondria. *PLOS Genet.* 10:e1004616
94. Takeuchi N, Nierhaus KH. 2015. Response to the Formal Letter of Z. Chrzanowska-Lightowlers and R. N. Lightowlers regarding our article "Ribosome rescue and translation termination at non-standard stop codons by ICT1 in mammalian mitochondria." *PLOS Genet.* 11:e1005218
95. Chrzanowska-Lightowlers ZM, Lightowlers RN. 2015. Response to "Ribosome rescue and translation termination at non-standard stop codons by ICT1 in mammalian mitochondria." *PLOS Genet.* 11:e1005227
96. Preuss M, Leonhard K, Hell K, Stuart RA, Neupert W, Herrmann JM. 2001. Mba1, a novel component of the mitochondrial protein export machinery of the yeast *Saccharomyces cerevisiae*. *J. Cell Biol.* 153:1085–96
97. Josyula R, Jin Z, Fu Z, Sha B. 2006. Crystal structure of yeast mitochondrial peripheral membrane protein Tim44p C-terminal domain. *J. Mol. Biol.* 359:798–804
98. Weiss C, Oppliger W, Vergères G, Demel R, Jenö P, et al. 1999. Domain structure and lipid interaction of recombinant yeast Tim44. *PNAS* 96:8890–94
99. Bauerschmitt H, Mick DU, Deckers M, Vollmer C, Funes S, et al. 2010. Ribosome-binding proteins Mdm38 and Mba1 display overlapping functions for regulation of mitochondrial translation. *Mol. Biol. Cell* 21:1937–44
100. Wilson DN. 2014. Ribosome-targeting antibiotics and mechanisms of bacterial resistance. *Nat. Rev. Microbiol.* 12:35–48
101. Schlünzen F, Zarivach R, Harms J, Bashan A, Tocilj A, et al. 2001. Structural basis for the interaction of antibiotics with the peptidyl transferase centre in eubacteria. *Nature* 413:814–21
102. Hansen JL, Ippolito JA, Ban N, Nissen P, Moore PB, Steitz TA. 2002. The structures of four macrolide antibiotics bound to the large ribosomal subunit. *Mol. Cell* 10:117–28
103. Denslow ND, O'Brien TW. 1978. Antibiotic susceptibility of the peptidyl transferase locus of bovine mitochondrial ribosomes. *Eur. J. Biochem.* 91:441–48
104. Zhang L, Ging NC, Komoda T, Hanada T, Suzuki T, Watanabe K. 2005. Antibiotic susceptibility of mammalian mitochondrial translation. *FEBS Lett.* 579:6423–27
105. Tu D, Blaha G, Moore PB, Steitz TA. 2005. Structures of MLSBK antibiotics bound to mutated large ribosomal subunits provide a structural explanation for resistance. *Cell* 121:257–70
106. Bidou L, Allamand V, Rousset J-P, Namy O. 2012. Sense from nonsense: therapies for premature stop codon diseases. *Trends Mol. Med.* 18:679–88
107. Borovinskaya MA, Pai RD, Zhang W, Schuwirth BS, Holton JM, et al. 2007. Structural basis for aminoglycoside inhibition of bacterial ribosome recycling. *Nat. Struct. Mol. Biol.* 14:727–32
108. Moazed D, Noller HF. 1987. Interaction of antibiotics with functional sites in 16S ribosomal RNA. *Nature* 327:389–94
109. Carter AP, Clemons WM, Brodersen DE, Morgan-Warren RJ, Wimberly BT, Ramakrishnan V. 2000. Functional insights from the structure of the 30S ribosomal subunit and its interactions with antibiotics. *Nature* 407:340–48
110. Hobbie SN, Bruell CM, Akshay S, Kalapala SK, Shcherbakov D, Böttger EC. 2008. Mitochondrial deafness alleles confer misreading of the genetic code. *PNAS* 105:3244–49

111. Hobbie SN, Akshay S, Kalapala SK, Bruell CM, Shcherbakov D, Böttger EC. 2008. Genetic analysis of interactions with eukaryotic rRNA identify the mitoribosome as target in aminoglycoside ototoxicity. *PNAS* 105:20888–93
112. Matt T, Ng CL, Lang K, Sha S-H, Akbergenov R, et al. 2012. Dissociation of antibacterial activity and aminoglycoside ototoxicity in the 4-monosubstituted 2-deoxystreptamine apramycin. *PNAS* 109:10984–89
113. Meyer M, Freihofer P, Scherman M, Teague J, Lenaerts A, Böttger EC. 2014. In vivo efficacy of apramycin in murine infection models. *Antimicrob. Agents Chemother.* 58:6938–41
114. Mace PD, Riedl SJ. 2010. Molecular cell death platforms and assemblies. *Curr. Opin. Cell Biol.* 22:828–36
115. Kissil JL, Deiss LP, Bayewitch M, Raveh T, Khaspekov G, Kimchi A. 1995. Isolation of *DAP3*, a novel mediator of interferon-γ-induced cell death. *J. Biol. Chem.* 270:27932–36
116. Ekert PG, Vaux DL. 2005. The mitochondrial death squad: hardened killers or innocent bystanders? *Curr. Opin. Cell Biol.* 17:626–30
117. Kissil JL, Cohen O, Raveh T, Kimchi A. 1999. Structure-function analysis of an evolutionary conserved protein, DAP3, which mediates TNF-α- and Fas-induced cell death. *EMBO J.* 18:353–62
118. Miyazaki T, Reed JC. 2001. A GTP-binding adapter protein couples TRAIL receptors to apoptosis-inducing proteins. *Nat. Immunol.* 2:493–500
119. Berger T, Brigl M, Herrmann JM, Vielhauer V, Luckow B, et al. 2000. The apoptosis mediator mDAP-3 is a novel member of a conserved family of mitochondrial proteins. *J. Cell Sci.* 113:3603–12
120. Berger T, Kretzler M. 2002. Interaction of DAP3 and FADD only after cellular disruption. *Nat. Immunol.* 3:3–5
121. Mukamel Z, Kimchi A. 2004. Death-associated protein 3 localizes to the mitochondria and is involved in the process of mitochondrial fragmentation during cell death. *J. Biol. Chem.* 279:36732–38
122. Berger T, Kretzler M. 2002. TRAIL-induced apoptosis is independent of the mitochondrial apoptosis mediator DAP3. *Biochem. Biophys. Res. Commun.* 297:880–84
123. Denslow ND, Anders JC, O'Brien TW. 1991. Bovine mitochondrial ribosomes possess a high affinity binding site for guanine nucleotides. *J. Biol. Chem.* 266:9586–90
124. Koc EC, Ranasinghe A, Burkhart W, Blackburn K, Koc H, et al. 2001. A new face on apoptosis: Death-associated protein 3 and PDCD9 are mitochondrial ribosomal proteins. *FEBS Lett.* 492:166–70
125. Erzberger JP, Berger JM. 2006. Evolutionary relationships and structural mechanisms of AAA+ proteins. *Annu. Rev. Biophys. Biomol. Struct.* 35:93–114
126. Walker JE, Saraste M, Runswick MJ, Gay NJ. 1982. Distantly related sequences in the α- and β-subunits of ATP synthase, myosin, kinases and other ATP-requiring enzymes and a common nucleotide binding fold. *EMBO J.* 1:945–51
127. Hanson PI, Whiteheart SW. 2005. AAA+ proteins: have engine, will work. *Nat. Rev. Mol. Cell Biol.* 6:519–29
128. Leipe DD, Koonin EV, Aravind L. 2004. STAND, a class of P-loop NTPases including animal and plant regulators of programmed cell death: multiple, complex domain architectures, unusual phyletic patterns, and evolution by horizontal gene transfer. *J. Mol. Biol.* 343:1–28
129. O'Brien TW, Denslow ND, Anders JC, Courtney BC. 1990. The translation system of mammalian mitochondria. *Biochim. Biophys. Acta* 1050:174–78
130. Miller JL, Cimen H, Koc H, Koc EC. 2009. Phosphorylated proteins of the mammalian mitochondrial ribosome: implications in protein synthesis. *J. Proteome Res.* 8:4789–98
131. Miller JL, Koc H, Koc EC. 2008. Identification of phosphorylation sites in mammalian mitochondrial ribosomal protein DAP3. *Protein Sci.* 17:251–60
132. Yoo YA, Kim MJ, Park JK, Chung YM, Lee JH, et al. 2005. Mitochondrial ribosomal protein L41 suppresses cell growth in association with p53 and p27Kip1. *Mol. Cell. Biol.* 25:6603–16
133. Chintharlapalli SR, Jasti M, Malladi S, Parsa KVL, Ballestero RP, González-García M. 2005. BMRP is a Bcl-2 binding protein that induces apoptosis. *J. Cell. Biochem.* 94:611–26
134. Conde JA, Claunch CJ, Romo HE, Benito-Martín A, Ballestero RP, González-García M. 2012. Identification of a motif in BMRP required for interaction with Bcl-2 by site-directed mutagenesis studies. *J. Cell. Biochem.* 113:3498–508

135. Sun L, Liu Y, Frémont M, Schwarz S, Siegmann M, et al. 1998. A novel 52 kDa protein induces apoptosis and concurrently activates c-Jun N-terminal kinase 1 (JNK1) in mouse C3H10T1/2 fibroblasts. *Gene* 208:157–66
136. Quigley DA, Fiorito E, Nord S, Van Loo P, Alnæs GG, et al. 2014. The 5p12 breast cancer susceptibility locus affects MRPS30 expression in estrogen-receptor positive tumors. *Mol. Oncol.* 8:273–84
137. Warner JR, McIntosh KB. 2009. How common are extraribosomal functions of ribosomal proteins? *Mol. Cell* 34:3–11
138. Skladal D, Halliday J, Thorburn DR. 2003. Minimum birth prevalence of mitochondrial respiratory chain disorders in children. *Brain* 126:1905–12
139. Boczonadi V, Horvath R. 2014. Mitochondria: impaired mitochondrial translation in human disease. *Int. J. Biochem. Cell Biol.* 48:77–84
140. Serre V, Rozanska A, Beinat M, Chretien D, Boddaert N, et al. 2013. Mutations in mitochondrial ribosomal protein MRPL12 leads to growth retardation, neurological deterioration and mitochondrial translation deficiency. *Biochim. Biophys. Acta* 1832:1304–12
141. Menezes MJ, Guo Y, Zhang J, Riley LG, Cooper ST, et al. 2015. Mutation in mitochondrial ribosomal protein S7 (MRPS7) causes congenital sensorineural deafness, progressive hepatic and renal failure and lactic acidemia. *Hum. Mol. Genet.* 24:2297–307
142. Emdadul Haque M, Grasso D, Miller C, Spremulli LL, Saada A. 2008. The effect of mutated mitochondrial ribosomal proteins S16 and S22 on the assembly of the small and large ribosomal subunits in human mitochondria. *Mitochondrion* 8:254–61
143. Hanahan D, Weinberg RA. 2011. Hallmarks of cancer: the next generation. *Cell* 144:646–74
144. Pavlides S, Whitaker-Menezes D, Castello-Cros R, Flomenberg N, Witkiewicz AK, et al. 2009. The reverse Warburg effect: aerobic glycolysis in cancer associated fibroblasts and the tumor stroma. *Cell Cycle* 8:3984–4001
145. Feron O. 2009. Pyruvate into lactate and back: from the Warburg effect to symbiotic energy fuel exchange in cancer cells. *Radiother. Oncol.* 92:329–33
146. Lamb R, Ozsvari B, Lisanti CL, Tanowitz HB, Howell A, et al. 2015. Antibiotics that target mitochondria effectively eradicate cancer stem cells, across multiple tumor types: treating cancer like an infectious disease. *Oncotarget* 6:4569–84
147. Järås M, Ebert BL. 2011. Power cut: inhibiting mitochondrial translation to target leukemia. *Cancer Cell* 20:555–56
148. Giglione C, Boularot A, Meinnel T. 2004. Protein N-terminal methionine excision. *Cell. Mol. Life Sci.* 61:1455–74
149. Lee MD, She Y, Soskis MJ, Borella CP, Gardner JR, et al. 2004. Human mitochondrial peptide deformylase, a new anticancer target of actinonin-based antibiotics. *J. Clin. Investig.* 114:1107–16
150. Spirina O, Bykhovskaya Y, Kajava AV, O'Brien TW, Nierlich DP, et al. 2000. Heart-specific splice-variant of a human mitochondrial ribosomal protein (mRNA processing; tissue specific splicing). *Gene* 261:229–34
151. Kohler R, Boehringer D, Greber B, Bingel-Erlenmeyer R, Collinson I, et al. 2009. YidC and Oxa1 form dimeric insertion pores on the translating ribosome. *Mol. Cell* 34:344–53
152. Wickles S, Singharoy A, Andreani J, Seemayer S, Bischoff L, et al. 2014. A structural model of the active ribosome-bound membrane protein insertase YidC. *eLife* 3:e03035
153. Pettersen EF, Goddard TD, Huang CC, Couch GS, Greenblatt DM, et al. 2004. UCSF Chimera—a visualization system for exploratory research and analysis. *J. Comput. Chem.* 25:1605–12
154. Yusupova G, Yusupov M. 2014. High-resolution structure of the eukaryotic 80S ribosome. *Annu. Rev. Biochem.* 83:467–86

RELATED RESOURCES

An introduction to the methodology of cryo-EM, the technique that provided the latest insights into the structural biology of mitoribosomes, was beyond the scope of this review. The interested reader may wish to consult the following articles and reviews.

1. Cheng Y. 2015. Single-particle cryo-EM at crystallographic resolution. *Cell* 161:450–57
2. Cheng Y, Grigorieff N, Penczek PA, Walz T. 2015. A primer to single-particle cryo-electron microscopy. *Cell* 161:438–49
3. Nogales E, Scheres SHW. 2015. Cryo-EM: a unique tool for the visualization of macromolecular complexity. *Mol. Cell* 58:677–89
4. Li X, Mooney P, Zheng S, Booth CR, Braunfeld MB, et al. 2013. Electron counting and beam-induced motion correction enable near-atomic-resolution single-particle cryo-EM. *Nat. Methods* 10:584–90
5. McMullan G, Faruqi AR, Clare D, Henderson R. 2014. Comparison of optimal performance at 300 keV of three direct electron detectors for use in low dose electron microscopy. *Ultramicroscopy* 147:156–63